Design and Implementation of Control System For Magnetic Suspension Device

by

Omar Carrasquillo

SUBMITTED TO THE DEPARTMENT OF MECHANICAL ENGINEERING IN PARTIAL FULFILLMENT OF THE REQUIREMENTS FOR THE DEGREE OF

BACHELOR OF SCIENCE IN MECHANICAL ENGINEERING

AT THE

MASSACHUSETTS INSTITUTE OF TECHNOLOGY

June 2011

Signature of Author: _____
Department of Mechanical Engineering
May 19, 2011

Certified by: _____
David L. Trumper
Associate Professor
Thesis Supervisor

Accepted by: _____
John H. Lienhard V
Samuel C. Collins Professor of Mechanical Engineering
Undergraduate Officer

Design and Implementation of Control System For Magnetic Suspension Device

by

Omar Carrasquillo

Submitted to the Department of Mechanical Engineering
on May 6, 2011 in Partial Fulfillment of the
Requirements for the Degree of Bachelor of Science in
Mechanical Engineering

ABSTRACT

The purpose of this thesis was to gain more knowledge and experience in the areas of modeling, dynamics, and applied control theory. A single-axis magnetic suspension device originally designed by Professor David Trumper for classroom demonstrations was chosen to improve the understanding of the previously mentioned topics. The dynamics of these types of systems provide interesting control challenges due to the nonlinear nature of its dynamics. As a result, designing of a control system for this device required the understanding and experimentation of two nonlinear controls techniques: linearization of the plant around an operating point, and feedback linearization. A combination of electromagnetic theory and experimentation was used to model the suspension actuator, and two different controllers were designed and implemented using the different controls methods.

Thesis Supervisor: David L. Trumper

Title: Associate Professor

ACKNOWLEDGEMENTS

I would like to thank my thesis supervisor and academic advisor Professor David L. Trumper for his guidance and support during my time at MIT. This past year has been particularly challenging due to coursework, thesis research, and graduate school decisions, and Professor Trumper has been a great advisor along the way. In particularly, I would like to thank him for pointing me in the right direction during the period of time I've been working on this thesis to make sure I would complete the goal. I would also like to thank Mohammad Imani Nejad, Dr. Harrison Chin, and Roberto Melendez for answering my questions regarding magnetic levitation and basic control theory.

In my personal life, I would like to thank my family, specially my parents, Diego and Vanessa, for their unconditional love and support throughout my life. Also, I would like to thank the Theta Deuteron Charge of Theta Delta Chi for being a constant source of support I know I can rely on. Additionally, I would like to thank Nancy Foen, Charlie De Vivero, Michael Munoz, Parhys Napier, Michael Fraser, Pablo Bello, and Javier Garcia for their incredible support and their help dealing with difficult situations.

TABLE OF CONTENTS

LIST OF FIGURES

Chapter 1: Introduction

The objective of this thesis was to improve my knowledge in feedback control systems by designing and implementing a controller for a naturally unstable system. For this purpose, a one-degree-of-freedom magnetic suspension system was chosen; the complexities due to the nonlinear force/current/gap relationship provide an interesting challenge from a control theory perspective. Many undergraduate control theory classes focus mostly on linear controllers, so when studying nonlinear systems one is taught the method of linearizing around operating points in order to use the linear control techniques. However, this approach is not optimal for this system because many applications of magnetic suspension require that the system can operate over large variations of air gap. Thus, we explored the use on feedback linearization, a type of nonlinear control technique, as an alternate way to control systems with large variations around operating points.

1.1 System Overview

The single degree of freedom magnetic suspension device studied in this thesis is described in great detail in [1] and [2]. It was originally constructed and developed by Professor David Trumper with his students at the University of North Carolina at Charlotte to be used as a classroom demonstration illustrating nonlinear control. The levitation system, consisting of a position sensor, a magnetic actuator and a controller, is shown in Figure 1 as a conceptual schematic. Figure 2 shows an actual photograph of the hardware.

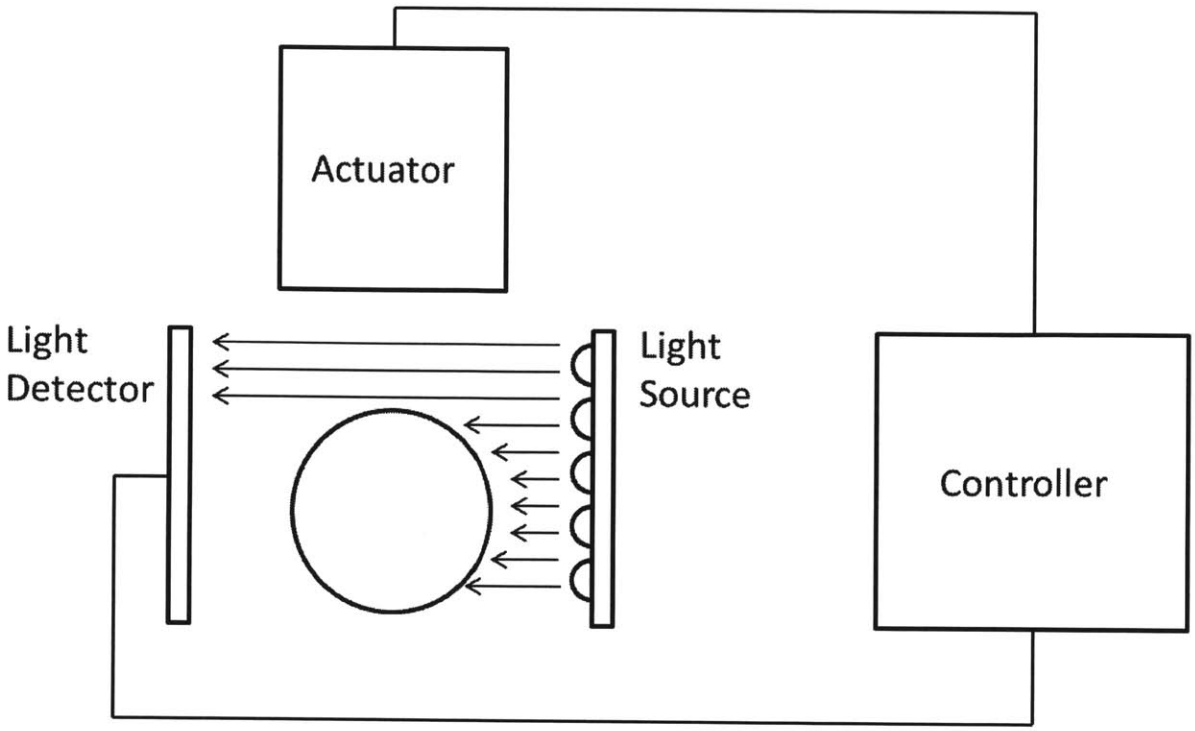

Figure 1: Conceptual schematic of magnetic suspension device.

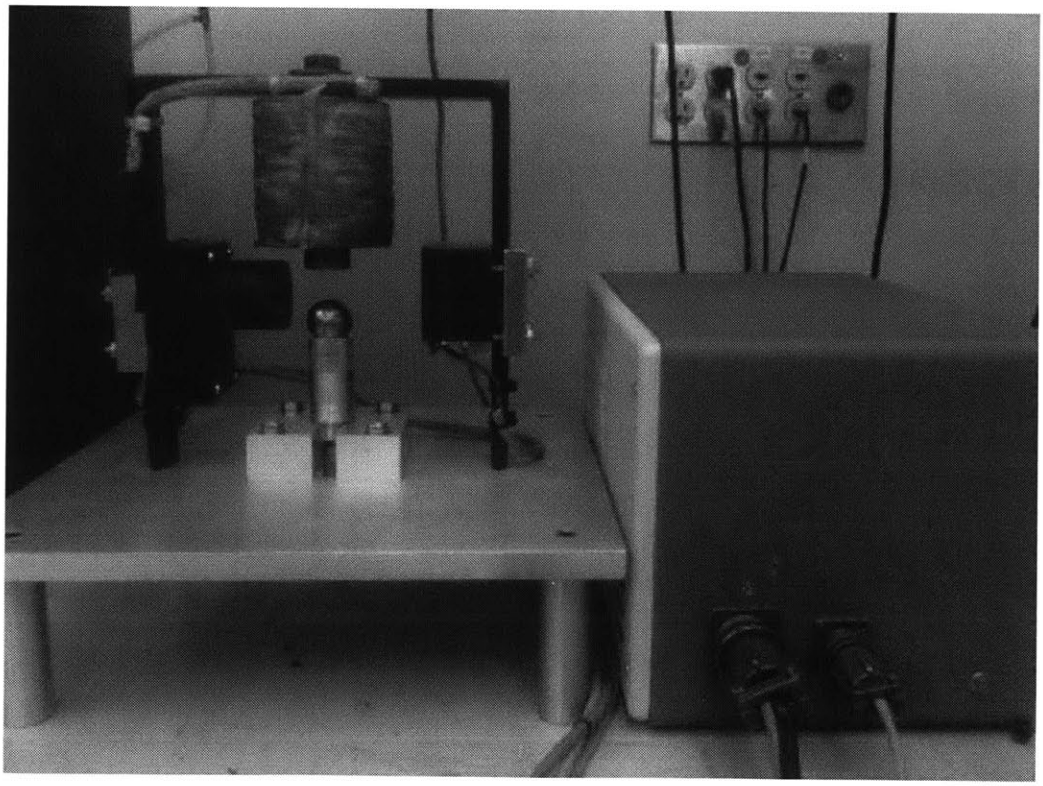

Figure 2: Photograph of physical hardware of magnetic suspension device

In this system, a steel ball of mass $m = 0.067$kg is suspended below a 2200-turn solenoid wound on a one inch steel core. This solenoid is an electromagnet whose field strength depends on the amount of current flowing through the coils at a given time, meaning that the electromagnet's magnetic force can be controlled by adjusting the current. This magnetic force can counteract the effect of gravity on the ball at a point of equilibrium. Hence, the vertical position of the ball can be actively controlled by manipulating the current flowing through the solenoid.

The other important part of the suspension system is the mechanism to detect the position of the ball. In this case, an optical sensor is used consisting of a light source and a photo detector. As the air gap between the ball and the pole of the electromagnet changes, so does the amount of light detected by the sensor. The controller correlates the amount of light detected by the sensor to the position of the ball and compares it to a reference input position, adjusting the magnetic force on the ball as needed by manipulating the current flow through the electromagnet. To calibrate the position sensor as well as characterize the nonlinear relationship between force, current, and air gap, a micrometer fixture, depicted in Figure 3 which was taken from [2], was used. Having these nonlinear equations, controllers were designed using two different approaches. One method involved linearizing the nonlinear equations about an operating point. The second approach used feedback linearization, which eliminates the operating point dependency and allows suspension over a wide range of air gaps. Both controllers were implemented and the systems response to step inputs were measured for both settings.

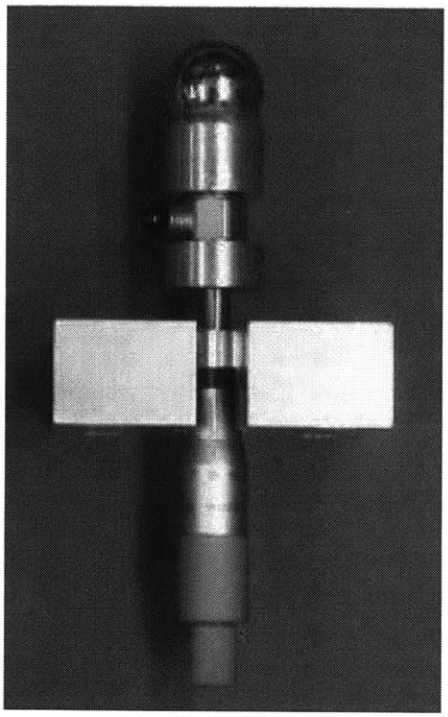

Figure 3: Photograph of the micrometer fixture. (Taken from [2])

1.2 Background

1.2.1 Linearized Model

In magnetic suspension systems, the nonlinearity emerges from the relationship between force, current, and air gap. In one approach, when nonlinear components are present, the system can be linearized about an operating point to yield a transfer function. As explained in [4], when a nonlinear equation is linearized, it is done so "for small-signal inputs about the steady-state solution when the small-signal input is equal to zero." This means that linearization of a system is limited to the region around the operating points, or points of equilibrium. After finding the equilibrium points, a Taylor series expansion is used to approximate the behavior of the system for a small range around these operating points.

1.2.2 Feedback Linearization

Feedback linearization is a technique that transforms a nonlinear system into a linear and controllable one. As described in [3], in the magnetic suspension application studied for this thesis, the complete nonlinear description of the electromagnetic field can be transformed into an apparent linear system. Hence, we could obtain consistent performance largely independent of the operating point air gap. After the system has been transformed, it is possible to use conventional linear feedback techniques to design a controller. Figure 4 shows a conceptual block diagram of a controller design using feedback linearization.

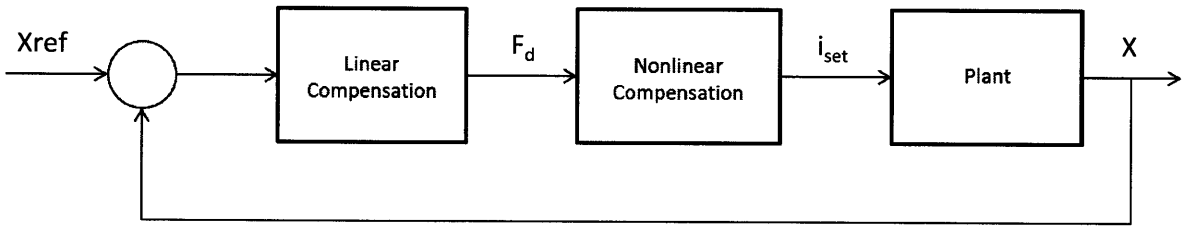

Figure 4: Block diagram of system with controller based on feedback linearization. (Taken from [2])

Chapter 2: Control Loop System

2.1 Introduction

A schematic representation of the magnetic suspension device was taken from [2] and is shows in Figure 5. The system consists of a position sensor, linear amplifier, digital controller, and actuator coil. The position sensor consists of a photodiode array illuminated by an array of light emitting diodes (LEDs). A steel ball is suspended between the LED light source and the detector and as its vertical position changes, so does the amount of light that enters the detector. Thus, the photodiode array produces a current proportional to the position of the steel ball. This current passes through a transresistance amplifier that converts the photodiode current to a voltage representative of position which can be fed into the computer. To control the actuator coil, a linear amplifier receives a voltage signal from the computer and produces a proportional current to drive the coil; hence, adjusting the magnetic force being applied to the steel ball.

The system is controlled via a desktop computer with a dSPACE board. We are able to communicate with the hardware using the dSPACE board in conjunction with MATLAB and Simulink software. Since Simulink supports block diagrams, a model of the compensated system is built on Simulink and downloaded onto the dSPACE board.

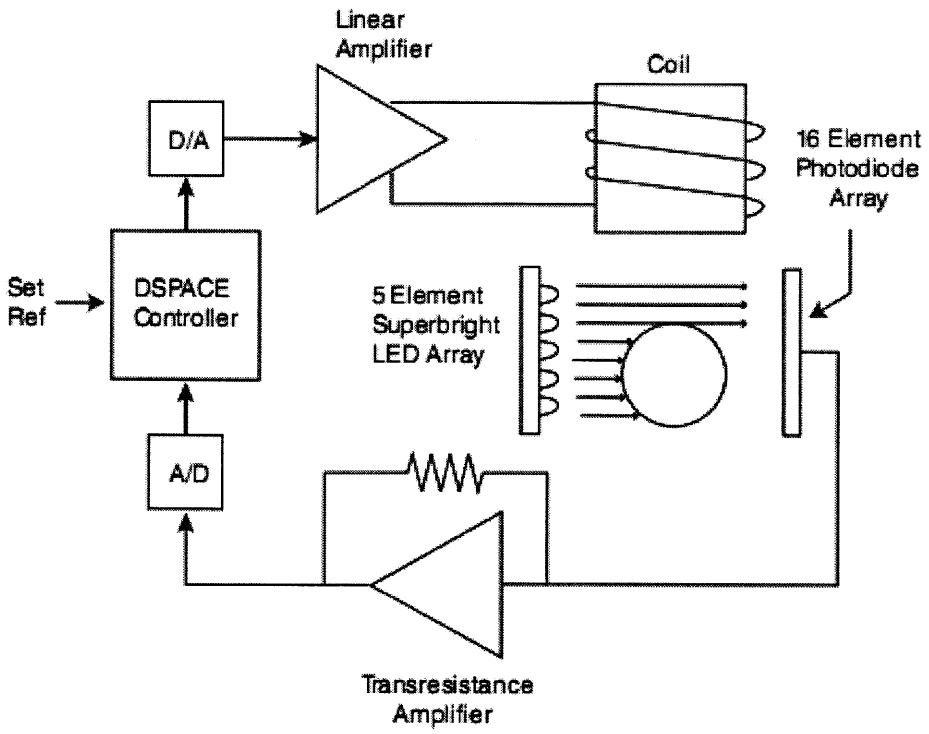

Figure 5: System control loop diagram. (Taken from [2])

2.2 Light Sensor

The magnetic suspension system uses a light sensor to determine the position of the suspended steel ball. The air gap we are trying to control is the distance between the coil and suspended ball. As the air gap decreases, the ball creates a shadow between the LED light source and the light sensor which decreases its current output and thus the voltage reading that comes into the dSPACE board. In order to determine the relationship between gap and voltage, a steel ball was attached to a micrometer and moved through the gap range while recording the voltage reading from the transresistance amplifier. The data is plotted in Figure 6. MATLAB was used to plot the data and find a cubic fit to describe the air gap corresponding to a voltage reading. This fit was used in the controller implementations in Simulink.

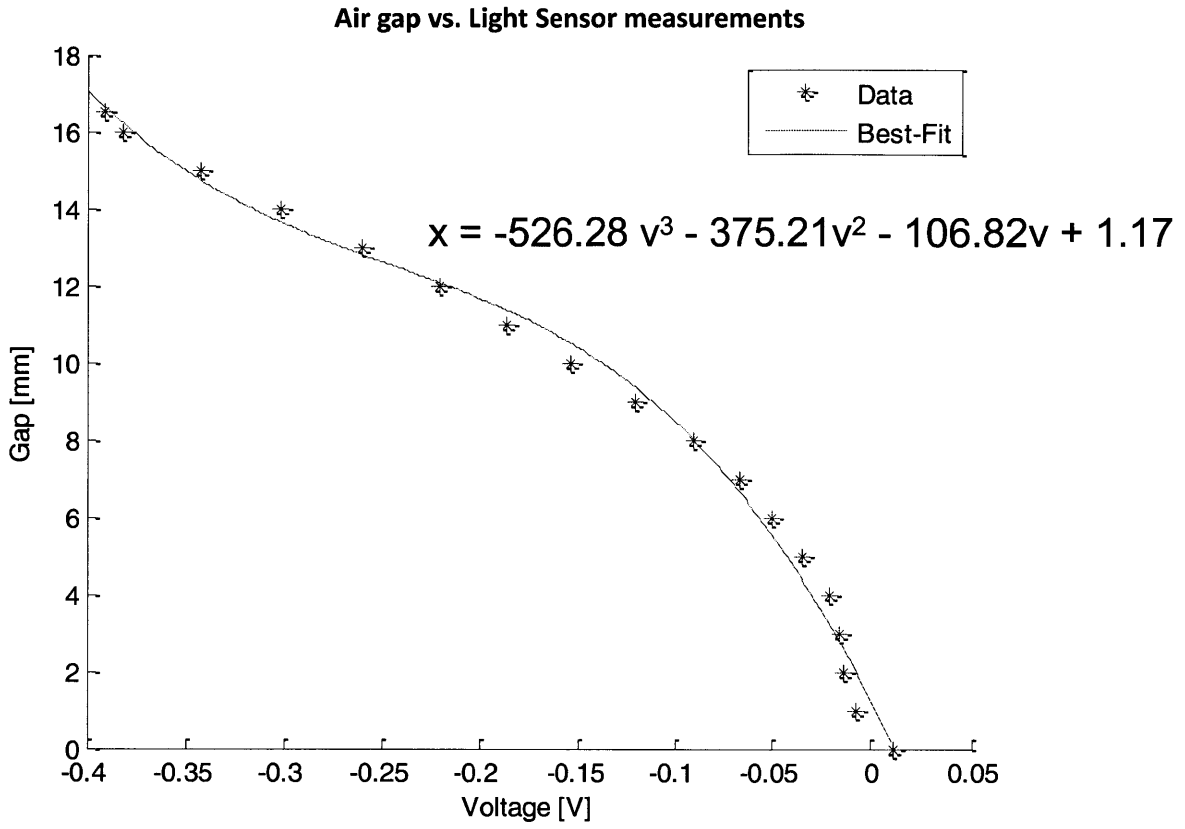

Figure 6: Plot of air gap vs. load sensor readings used to calibrate the position sensor. Data interpolated with a cubic fit.

2.3 Actuator Coil

2.3.1 Source of Data

In order to have a good understanding of the relationship between the current flowing through the coil, the magnetic force it executes on the steel ball and the air gap, it was necessary to run a series of tests. In past works, like those explained with great detail in [1], [2] and [5], a piezo-electric load cell attached to the steel ball in the micrometer structure shown in Figure 3 was used to measure the force applied by the actuator coil, for an applied current, on the steel ball at a given air gap. Due to time limitations, data from these sources was used in the present work.

2.3.2 Actuator Model

The equation that describes the force produced by an electromagnet, as taken from [2] is

$$F = C\left(\frac{i}{x}\right)^2, \tag{1}$$

where F is the force applied to the ball, i is the current through the coil, and x is the air gap, the distance between the pole of the electromagnet and the steel ball. The constant C (Nm^2/A^2) depends on material properties and physical structure and it must be determined experimentally. In addition, it is important to note that in this model, the gap length is increasing in the downward direction, meaning that at large values of x, the ball is far from the pole of the electromagnet.

In [2], Yi Xie provides great details about the nonidealities of the system that are not taken into account in Equation 1. From these, it is important to highlight that the ideal case assumes that all the magnetic flux is concentrated in the air gap. Using a magnetic circuit analogy to this system, Yi Xie explains that the ideal model suggests an infinite force on the ball with zero air gap space. Taken this into account, a constant factor, x_0, is added to the gap length in the denominator of Equation 1 so that the force approaches a finite value as the air gap approaches zero. The new equation is

$$F = C\left(\frac{i}{x + x_0}\right)^2. \tag{2}$$

Both x_0 and C were found experimentally in [2]. They were reported to be

$$x_0 = 0.0025\, m, \tag{3}$$

and

$$C = -0.003x + 6.54\times10^{-4}\frac{Nm^2}{A^2}. \tag{4}$$

In [2] and in [5] the force-current-gap data was measured experimentally using the micrometer fixture with the piezo-electric load cell. As different amounts of current were passed through the coil, the magnetic force on the steel ball was recorded at different air gaps. Figure 7, which was taken from [5], shows the force-current relationship measured at 7mm gap as well as the model described by Equation 2. It can be seen that the model is not accurate after currents of 0.4A. In [2], careful experimentation and trial and error led to a higher order model which models the force-current relationship more accurately at a particular gap. This higher order model is shown in Equation 5 and was also included in Figure 7.

$$i = (x + x_0)\sqrt{\frac{F}{C}} + F\left(0.0195e^{\frac{x-0.002}{0.006}} - 3.5(x - 0.007)\right) + 450(x - 0.0014)^2 F^2. \tag{5}$$

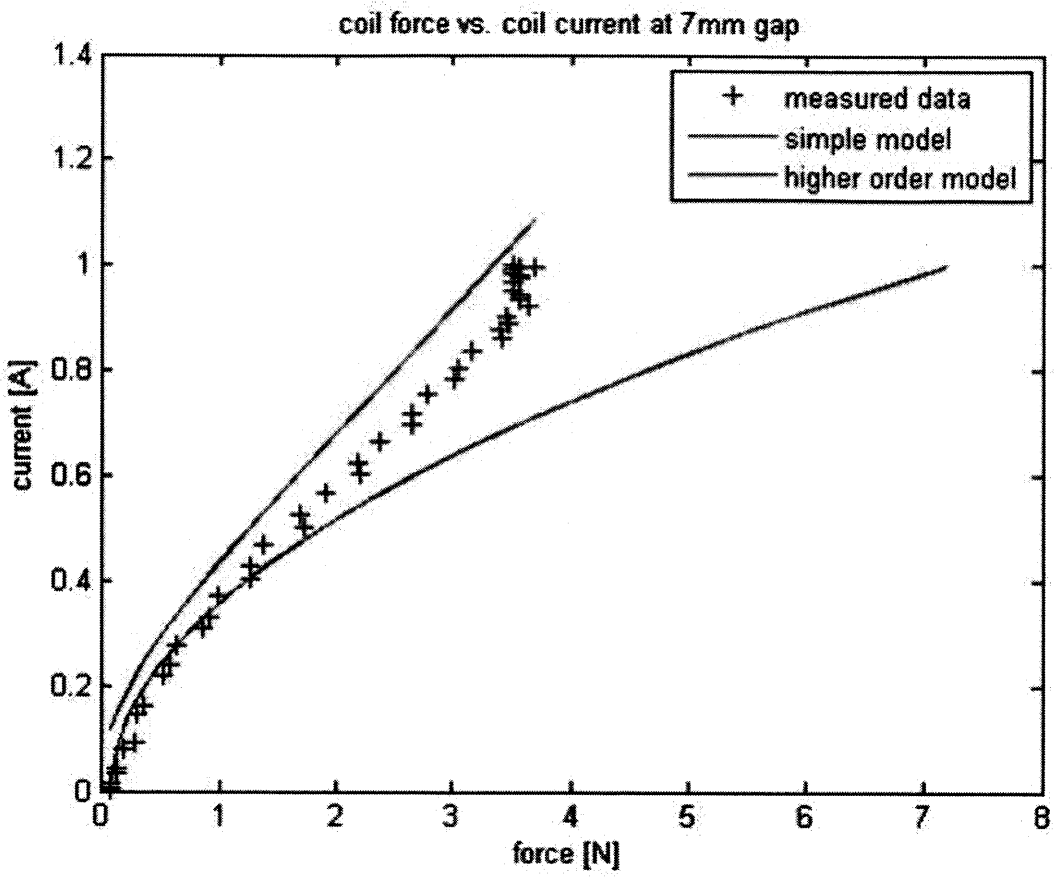

Figure 7: Measured and modeled force-current relationships at 7mm gap. (Taken from [5])

Chapter 3: Nonlinear Control Techniques

3.1 Linearization

3.1.1 System Dynamics

The concept behind magnetic suspension is to use the magnetic force created by the electromagnet to counteract the effect of gravity on the steel ball; hence, when these two forces are balanced, there is a point of equilibrium. A way to solve this control problem is to linearize the system around these equilibrium, or operating, points and use traditional linear control techniques. In order to linearize the system, we have to use a first-order Taylor series expansion to approximate the behavior of the system over a limited range around the operating points. After analyzing the free-body diagram of the system, shown in Figure 8, we can find the equilibrium points by balancing the forces in the vertical direction.

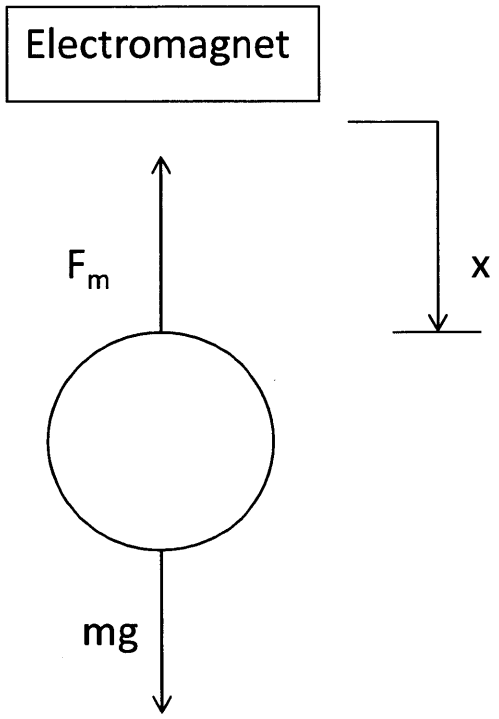

Figure 8: Free-body diagram of steel ball under suspension.

Sum of forces in the vertical direction yields

$$m\ddot{x} = mg - F_m . \tag{6}$$

Substituting for the magnetic force, we can rewrite Equation 6 as

$$m\ddot{x} = mg - C\left(\frac{i}{x}\right)^2 . \tag{7}$$

Looking at Equation 7, we can see the nonlinear term which depends on current and air gap. Thus, we need to linearize the system about these two variables by taking a first-order Taylor series expansion about points that describe a desired operating point and small deviations from:

$$\begin{aligned} i &= \bar{i} + \tilde{i} \\ x &= \bar{x} + \tilde{x} \end{aligned} . \tag{8}$$

In Equation 8, the bar denotes the equilibrium operating point and tilde represents small deviations from the operating point. Applying a first order approximation of the Taylor series expansion of the magnetic force gives

$$F_m = C\left(\frac{\bar{i}}{\bar{x}}\right)^2 + \left.\frac{\partial F}{\partial x}\right|_{\bar{i},\bar{x}} \tilde{x} + \left.\frac{\partial F}{\partial i}\right|_{\bar{i},\bar{x}} \tilde{i} \tag{9}$$

Solving the partial differential equations, we get

$$\begin{aligned} \left.\frac{\partial F}{\partial x}\right|_{\bar{i},\bar{x}} \tilde{x} &= -2C\frac{\bar{i}^2}{\bar{x}^3}\tilde{x} \\ \left.\frac{\partial F}{\partial i}\right|_{\bar{i},\bar{x}} \tilde{i} &= 2C\frac{\bar{i}}{\bar{x}^2}\tilde{i} . \end{aligned} \tag{10}$$

For simplicity, we will assign the following constants:

$$\begin{aligned} k_1 &= 2C\frac{\bar{i}^2}{\bar{x}^3} \\ k_2 &= 2C\frac{\bar{i}}{\bar{x}^2} . \end{aligned} \tag{11}$$

To find the point of equilibrium or the system, we know the sum of forces in the vertical must equal zero. This means that at the operating point,

$$mg = C\left(\frac{\bar{i}}{\bar{x}}\right)^2. \tag{12}$$

Combining Equations 7-12, we yield the final differential equation representing the linearized system:

$$m\ddot{x} = k_1 \tilde{x} - k_2 \tilde{i}. \tag{13}$$

Now, we can find the transfer function of the system that describes the air gap as a result of the current input by taking the Laplace transform of the linearized differential equation and rearranging some terms:

$$\frac{X(s)}{I(s)} = \frac{-k_2}{ms^2 - k_1}. \tag{14}$$

Analyzing the transfer function in Equation 14, we can see that the system is open loop unstable due to a pole in the right hand side of the complex plane. Thus, controller compensation has to move the unstable pole into the stable left-half plane region.

3.1.2 Controller Design

In order to stabilize our system, we implemented a lead compensator with the form

$$G_c(s) = K\frac{\alpha\tau s + 1}{\tau s + 1}. \tag{15}$$

A lead compensator allows us to add phase to the uncompensated system in the neighborhood of the crossover frequency. We chose to place the compensator's pole and zero a decade a part, meaning $\alpha = 10$. For the controller design, we will choose a crossover frequency of 10 Hz (62.8 rad/s). To determine the parameters of the lead compensator, we will look at the plant's Bode plot, shown in Figure 9, to see how we need to compensate the system to make it stable.

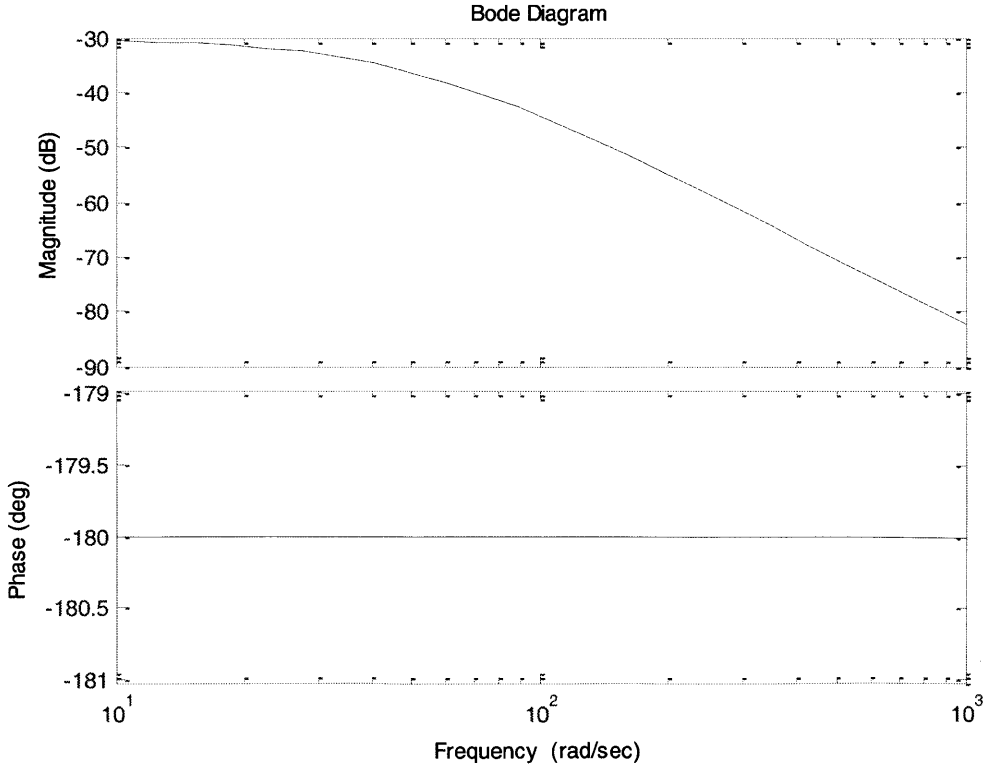

Figure 9: Bode plot for linearized plant transfer function (Equation 14).

At the chosen crossover frequency of 62.8 rad/s, the magnitude of the uncompensated plant is 0.0118. In addition, we see that the plant's phase is -180° for all frequencies.

For the design of the lead compensator parameters we observe the system's loop transmission:

$$L.T. = -Kk_2 \frac{\alpha\tau s + 1}{(ms^2 - k_1)(\tau s + 1)}. \tag{16}$$

We want the loop transmission to have a phase margin of at least 45° for good stability and a magnitude equal to 1. This requirements mean that the phase of the loop transmission at the crossover frequency must be less than or equal to -135° and the magnitude must be 1 at this frequency. From Equation 15, it can be determined that the zero is located at $\frac{-1}{\alpha\tau}$ and the pole at $\frac{-1}{\tau}$. The maximum phase of a lead compensator occurs at the geometric mean of the pole and zero break frequencies, which in this case occurs at

$$\omega_c = \frac{1}{\sqrt{\alpha}\,\tau}, \tag{17}$$

where ω_c is the crossover frequency. Given that we set $\alpha = 10$, and $\omega_c = 62.8$ rad/s, we find that $\tau = 0.005$ s. The proportional gain K is determined from the condition of having unity loop transmission at the crossover frequency. Knowing that the magnitude of a lead compensator is equal to $K\sqrt{\alpha}$ at the crossover frequency, we set unity magnitude of the loop transmission by

$$K\sqrt{\alpha}(0.0118) = 1 \quad \Rightarrow K = 27. \tag{18}$$

Figure 10 shows the theoretical loop transmission Bode plot and Figure 11 shows the step response of the closed-loop system.

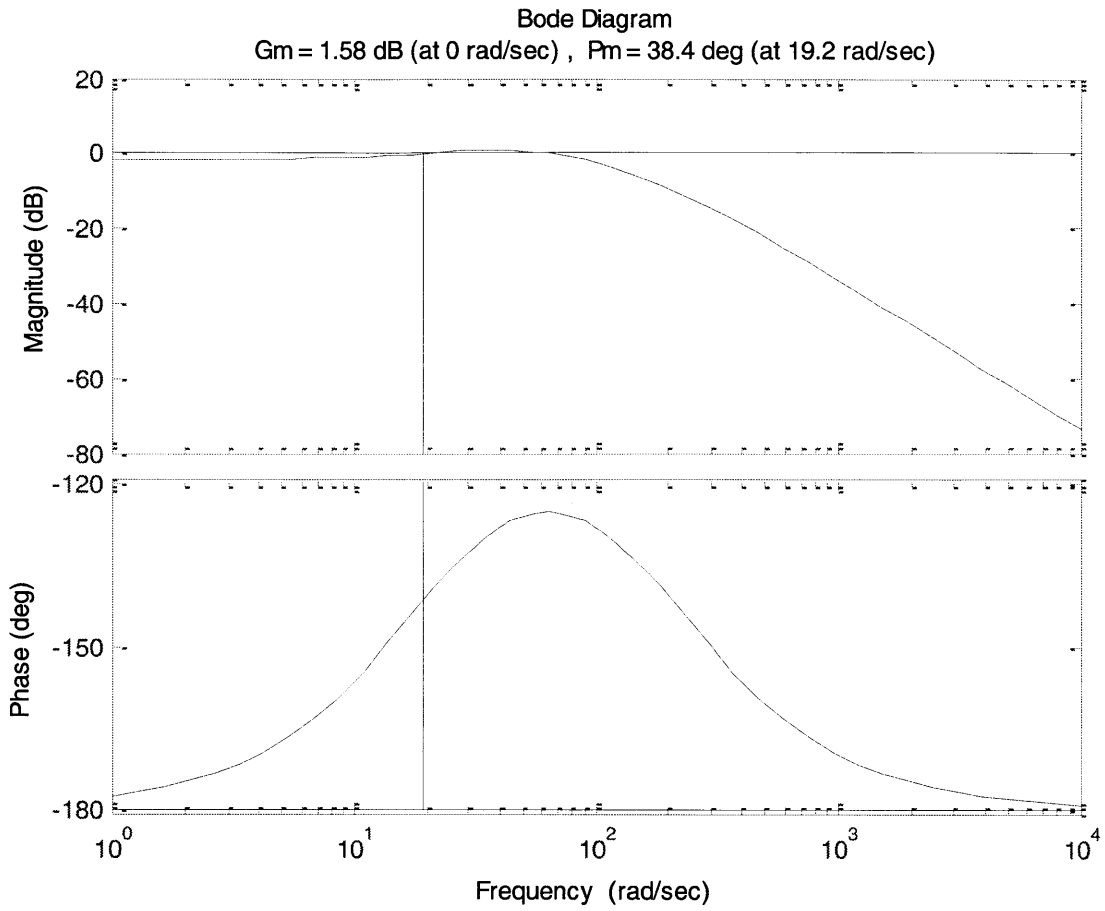

Figure 10: Simulated Bode plot for loop transmission of linearized system with model given by Equation 15 with K=27, $\alpha = 10$, and $\tau = 0.005$.

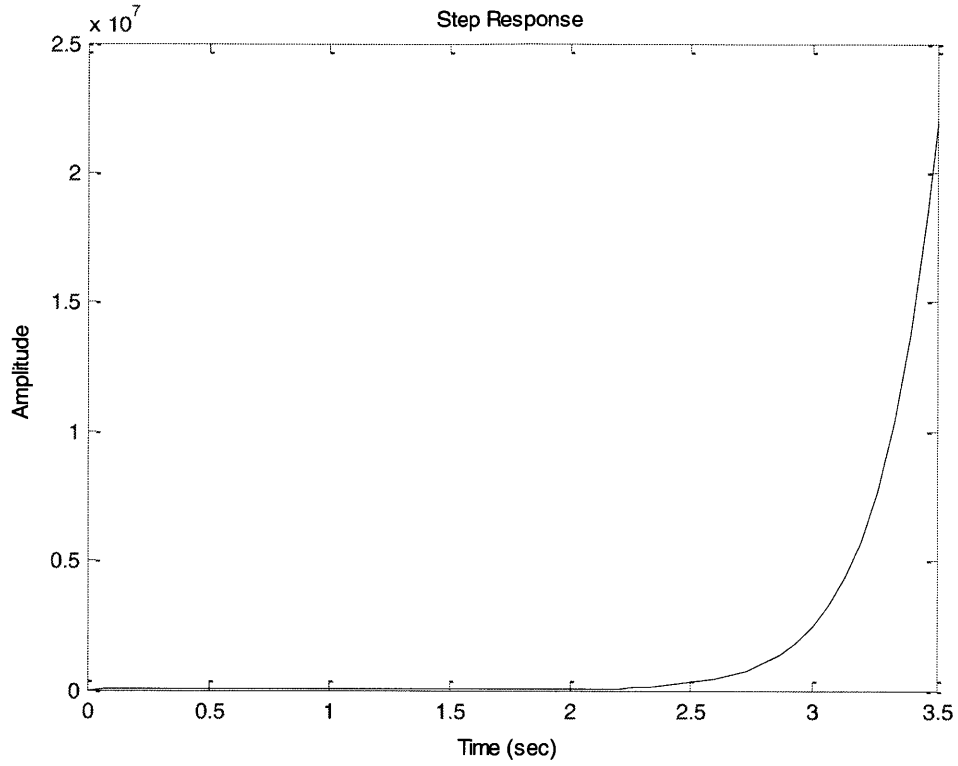

Figure 11: Simulated closed loop step response of linearized system with lead compensation in the forward path; model given by Equation 15 with K = 27, α = 10, and τ=0.005.

The design parameters were not chosen correctly because this system is still unstable, with a phase margin of just 38.4° at 19.2 rad/s. A possible explanation for this is that our chosen crossover frequency of 10 Hz was too low. Looking back at the plant's frequency response from Figure 9, at 10 Hz the plant's magnitude hasn't really started to decay. This can be seen clearer in Figure 10, where it appears to be multiple crossover frequencies. Thus, to guaranty stability, we chose a much higher crossover frequency of 140 rad/s. Keeping the compensator's pole and zero a decade apart, Equation 17 yields $\tau = 0.0023$. In addition, Equation 18 yields a proportional gain $K = 92$.With this new parameters, the new theoretical loop transmission Bode plot was drawn and shown in Figure 12 and the closed loop step response is in Figure 13.

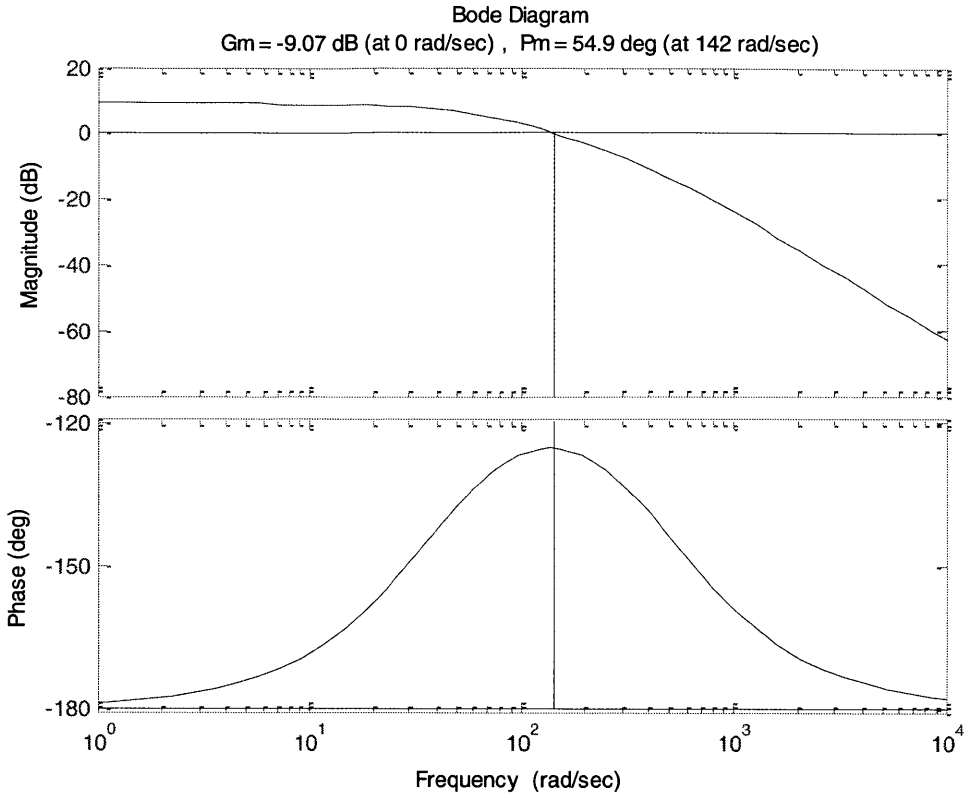

Figure 12: Simulated Bode plot for loop transmission of linearized system with model given by Equation 15 with K=92, $\alpha = 10$, and $\tau = 0.0023$.

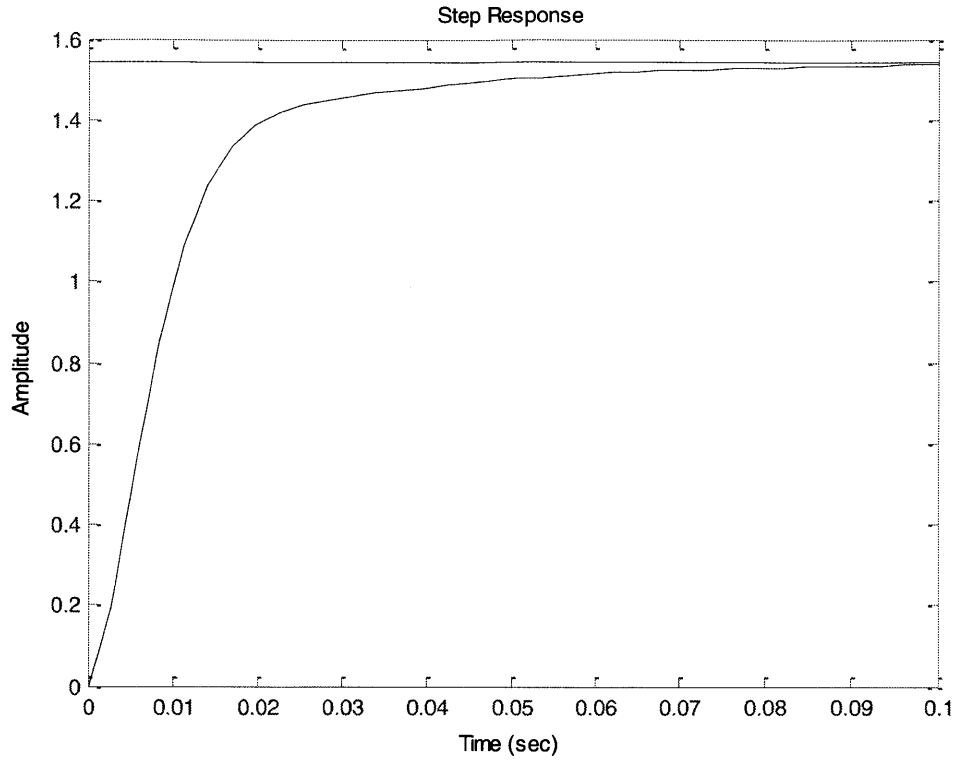

Figure 13: Simulated closed loop step response of linearized system with lead compensation in the forward path; model given by Equation 15 with K = 92, α=10, and τ = 0.0023.

With the new controller, there is phase margin of 54.9° at a crossover frequency of 140 rad/s. This system appears capable of stabilizing our system but it can still be improved. First, Figure 12 shows the system's magnitude to be relatively constant before reaching crossover and it is too close to 0 dB. Secondly, the system's step response shows a steady-state error. To address this, we designed a lag compensator with an integrator that would provide higher again at low frequencies as well as eliminate steady-state error. To avoid negative phase contributions from the lag compensator at crossover, the lag zero was placed roughly a decade before crossover frequency. Thus, we place the lag zero at 10 rad/s and the pole at the origin. The simulated frequency and step responses are shown in Figure 14 and Figure 15, respectively.

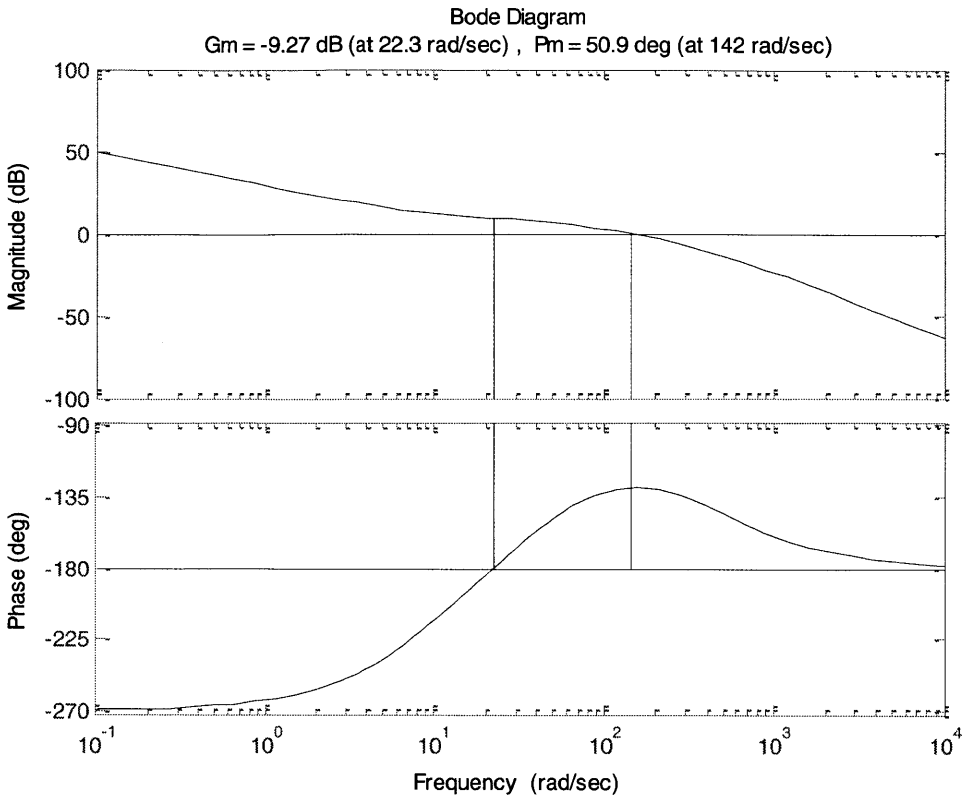

Figure 14: Simulated Bode plot for loop transmission of linearized system with lead and lag compensation in the forward path.

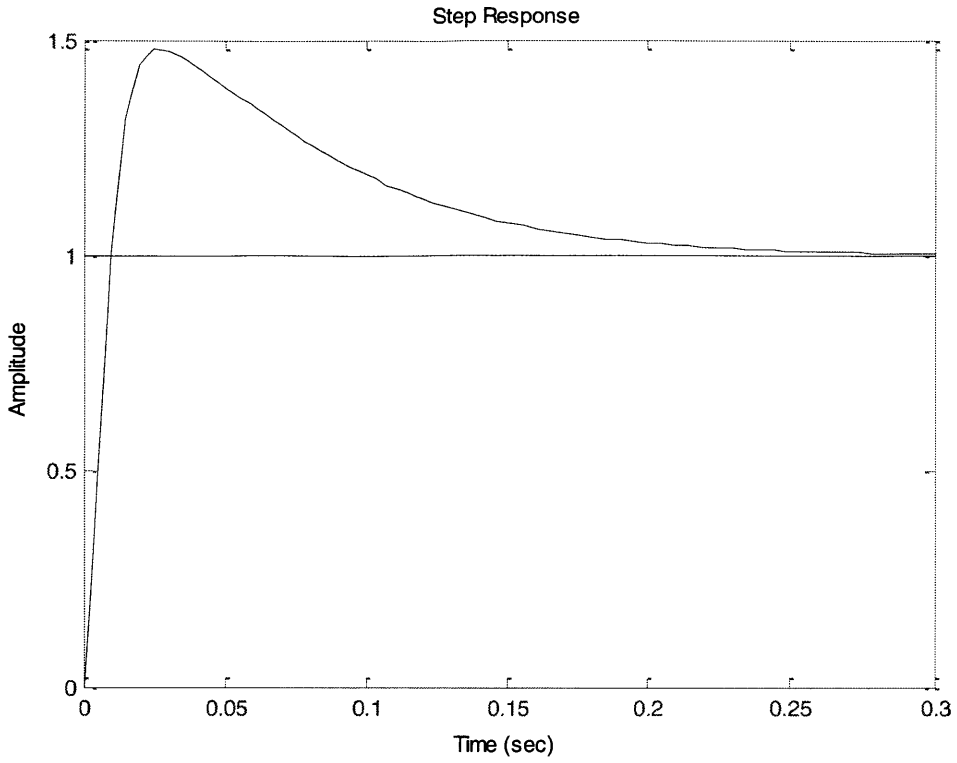

Figure 15: Simulated closed loop step response of linearized system with lead and lag compensation in the forward path.

As seen in Figure 14, the crossover frequency is now better defined. Also, the step response for the closed loop system chose no steady-state error, despite a high overshoot of approximately 50%. To attempt and reduce this overshoot, we decided to move the lead compensator from the forward path to the feedback path of the control loop. This change does not change the loop transmission behavior but changes closed loop dynamics. New simulated step response of the system with the lead compensator in the feedback path and the lag compensator in the forward path is shown in Figure 16.

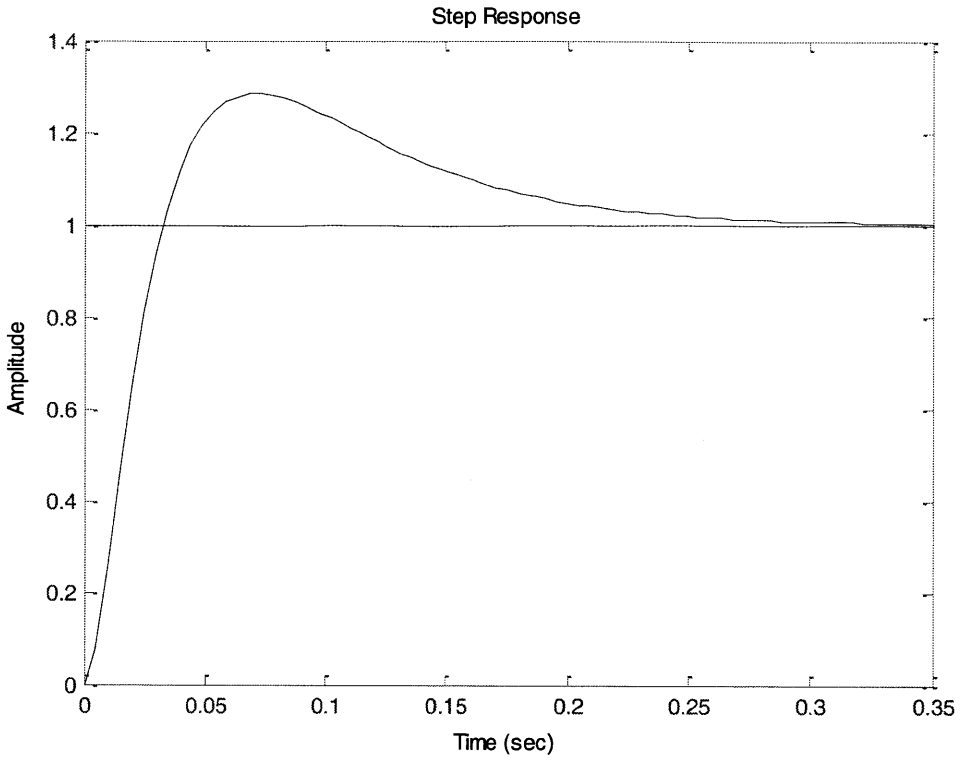

Figure 16: Simulated closed loop step response of linearized system with lead compensation in feedback path and lag compensation in the forward path.

3.1.3 Controller Implementation

The lead and lag compensators were implemented into the system through Simulink, MATLAB, and the dSPACE board. Figure 17 shows the Simulink model used for the controlling the linearized system. There is a transformation block at the input which converts the voltage readings into gap length using the cubic fit found when calibrating the light sensor. After configuring the physical controller view dSPACE, we noticed that there were discrepancies between the simulated system dynamics and the physical responses. We were attempting to stabilize the steel ball at a gap of 8 mm, but noticed the gain of 92 was too high and making the system go unstable. Thus, through trial and error, it was determined that a gain of 50 was very fit for the physical dynamics of the system. In order to test the behavior of the controller, we measured the step responses of the system to a 0.5mm input at different operating points. While measuring these responses, we noticed that the system was extremely noisy. In order to attenuate the noise and get higher quality data, a low-pass filter was designed and implemented.

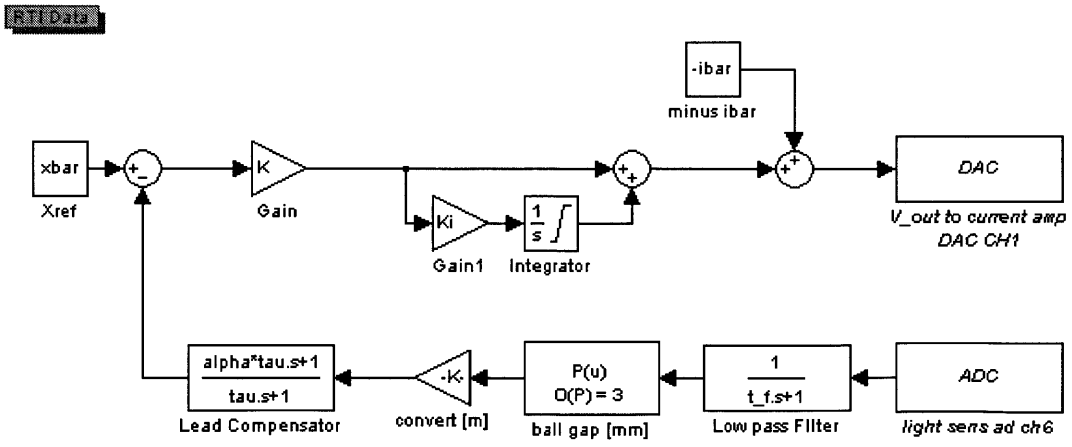

Figure 17: Simulink block diagram used to implement the linear controller for the linearized system around an operating point, *xbar*.

These measurements of step responses were taken directly from the voltage readings of the light sensor and converted to gap distance using the determined calibration. It can be seen that the system responses are very noisy and the ball is constantly oscillating about its operating point. Due to lack of time, this unexpected behavior could not be explored further. This oscillatory motion made it difficult to precisely determine the range of stability of the system because the system was not behaving optimally. Figures 18, 19, and 20 show the system's position responses to a 0.5 mm step at air gaps of 6 mm, 7 mm, 8 mm, 9 mm, and 10 mm. Through experimentation, we noticed that different air gaps required different gains for stability. Beyond an air gap of 11mm, the gain had to be increased in order to maintain stability; in the region of 12 mm gap, system required gain of over 125. Thus, we determined that the linear controller is stable for air gaps between 5 mm and 11 mm.

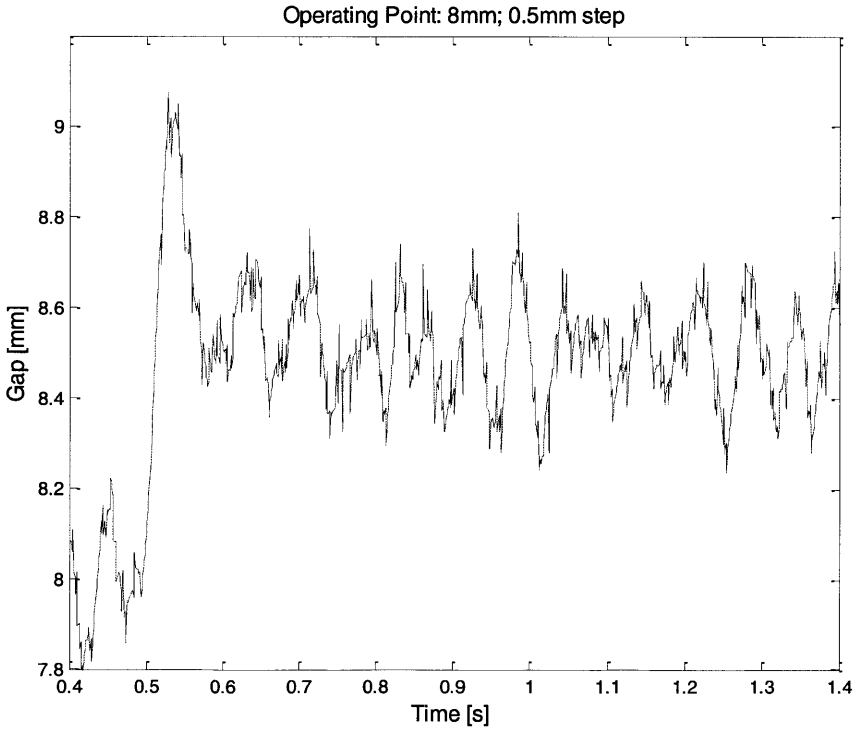

Figure 18: Position response as calculated from position sensor voltage measurement to a 0.5 mm step at 8 mm air gap (Linearized).

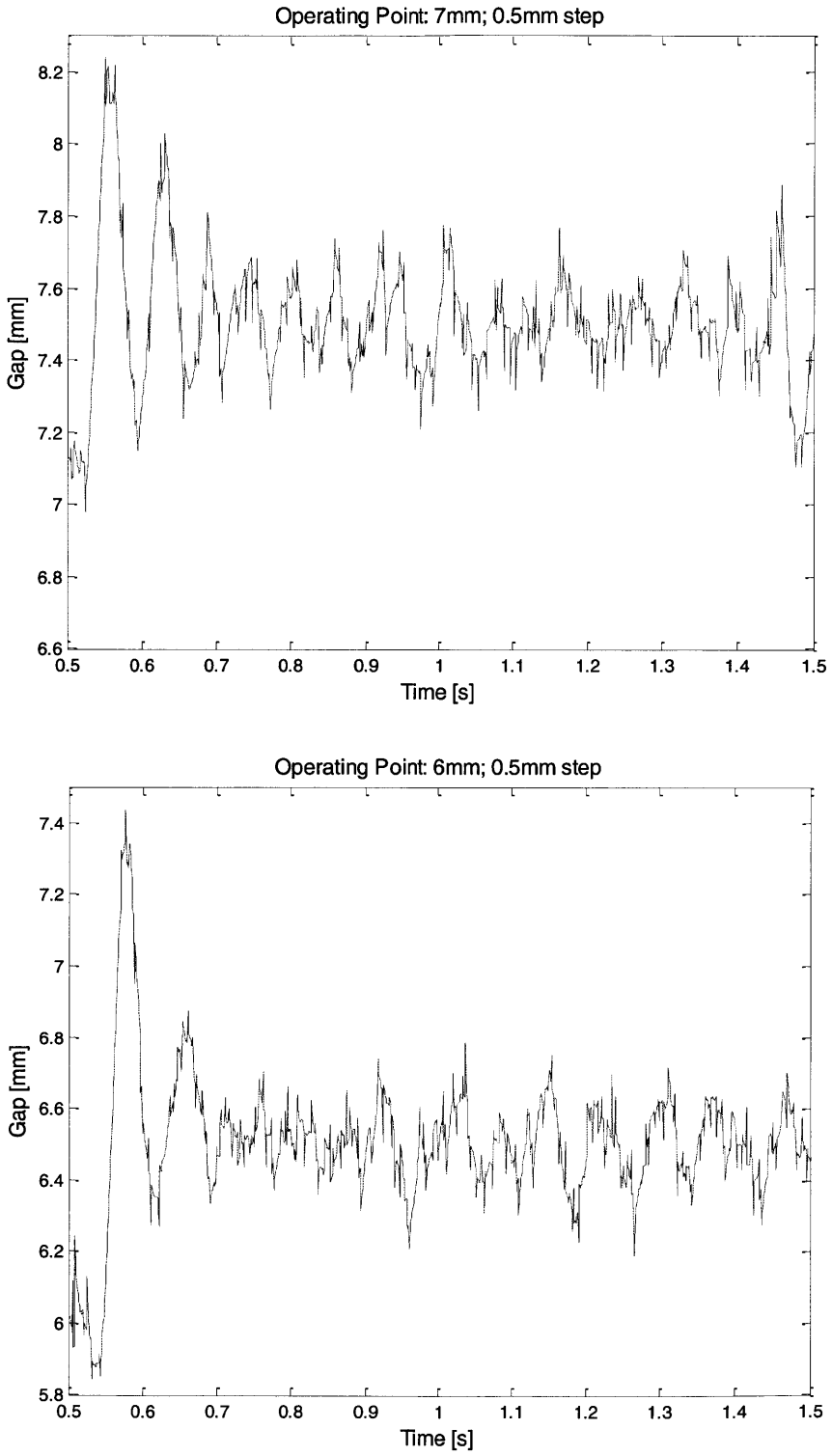

Figure 19: Position response as calculated from position sensor voltage measurement to a 0.5 mm step at 7 mm and 6 mm air gaps (Linearized).

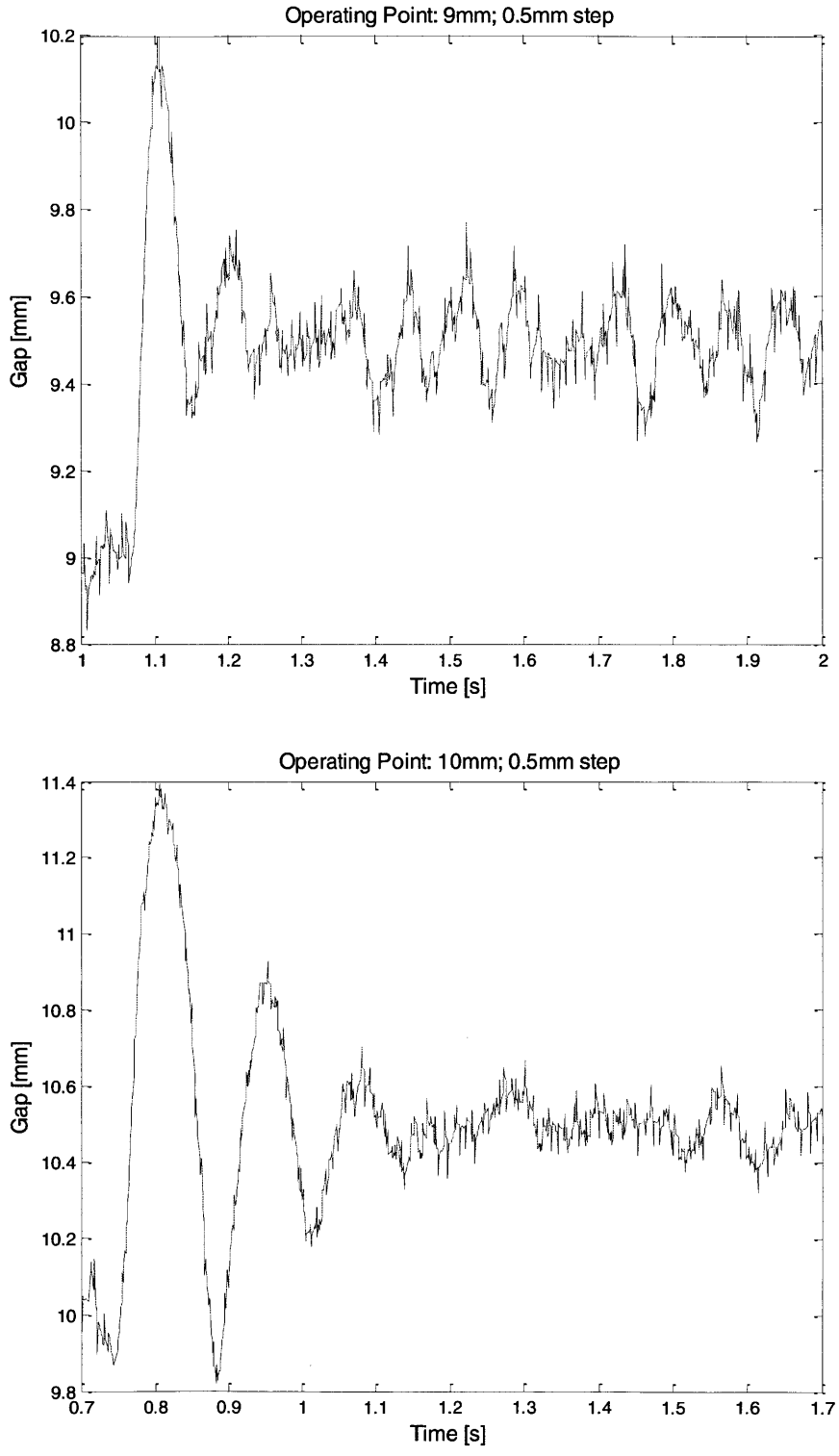

Figure 20: Position response as calculated from position sensor voltage measurement to a 0.5 mm step at 9 mm and 10 mm air gaps (Linearized).

3.2 Feedback Linearization

3.2.1 Theory

The design of a controller based on feedback linearization requires an accurate relationship between the current in the coil, magnetic force on the steel ball, and the air gap between the pole of the electromagnet and the ball. This method allows the controller to be valid over the entire operating range because the nonlinear transformation allows the system to calculate in real time the required current from a desired magnetic force at an instantaneous gap. This transformation is shown schematically in Figure 4, where the block labeled "Nonlinear Compensation" takes the desired force and instantaneous ball gap as inputs and outputs the desired current. Thus, feedback linearization allows us to use typical linear feedback techniques to design the controller because the software is making the nonlinearity look linear for all operating points.

The necessary characterization for calculating the current output as a result of the desired magnetic force can be found by rearranging Equation 1 to get

$$i = x\sqrt{\frac{F_d}{C}}, \tag{19}$$

where F_d is the desired magnetic force, x is the air gap, i is the current output to the coil and C is the constant found experimentally in Section 2.3.2. However, as discussed also in Section 2.3.2 of this work, Equation 19 is only accurate for small levels of current. Thus, for this controller we used the higher order relationship from Equation 5.

3.2.2 Controller Design

As discussed, feedback linearization in this suspension system allows for the combination of the nonlinear compensation block with the plant to appear linear over the entire range of air gaps to the linear compensation block. As seen in Figure 4, if the nonlinear compensator and the plant are taken as one, its input is the desired magnetic force and it outputs the desired air gap length. Thus, they can be collectively described by the transfer function

$$\frac{X(s)}{F(s)} = \frac{1}{ms^2}, \tag{20}$$

meaning that the system is marginally stable. Hence, the goal of the controller design is to move these poles far away from the origin and into the left-hand stable plane.

Similar to the linearized system, a lead compensator was used to stabilize the plant. Figure 21 shows the Bode plot of the model based on feedback linearization (Equation 20) which has aof -180°. A phase margin greater than 45° can be achieved through successful implementation of a lead compensator. For the design of the lead compensator parameters, we assume the compensator is in the forward path of the loop and we observe the system's loop transmission:

$$L.T. = K\frac{\alpha\tau s + 1}{ms^2(\tau s + 1)}. \tag{21}$$

For this controller, the crossover frequency was chosen to be 10 Hz (62.8 rad/s). Keeping the zero and pole of the lead compensator a decade apart (α=10), Equation 17 was used to find τ = 0.005. The proportionality gain K was found through the use of Equation 18 with the difference that the plant's magnitude at the crossover frequency is now 0.0038. Thus, K = 83.

Figure 22 shows the theoretical loop transmission Bode plot of the feedback linearized system with lead compensation and Figure 23 shows its closed-loop step response. The phase

margin is 54.9° at crossover, which is more stable than we had anticipated while designing the controller. Looking at the step response in Figure 23, despite the overshoot, the system is well damped and appears to have no steady-state error.

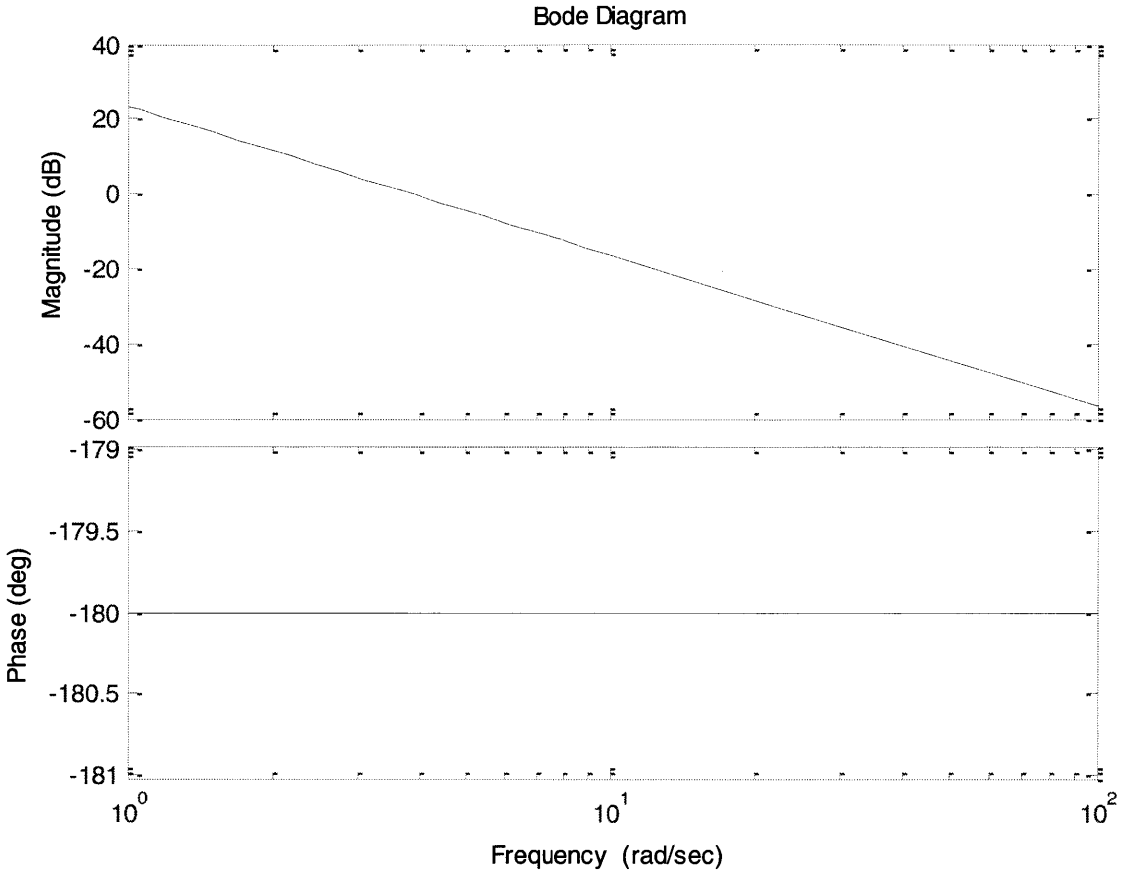

Figure 21: Simulated Bode plot for plant transfer function with feedback linearization based on Equation 20.

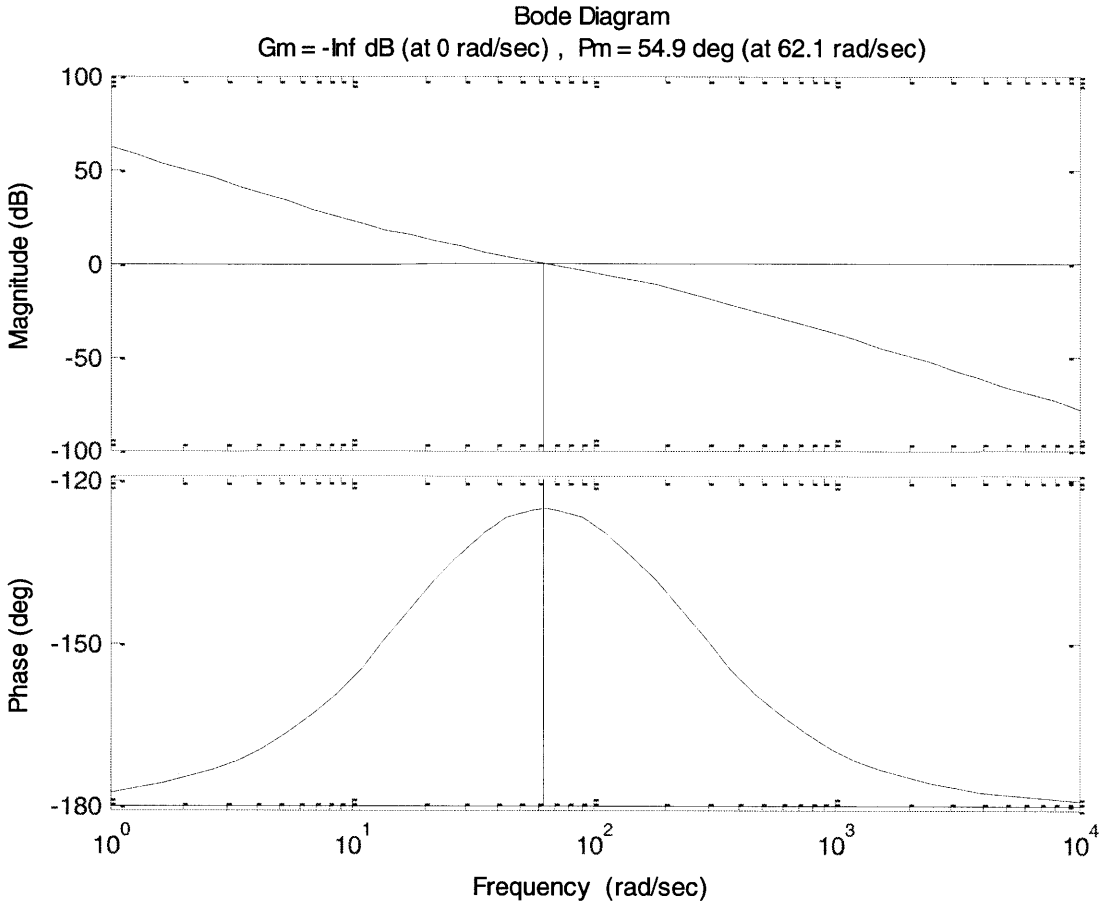

Figure 22: Simulated Bode plot for loop transmission of feedback linearized system with lead compensation; model given by Equation 15 with K=83, $\alpha = 10$, and $\tau = 0.005$.

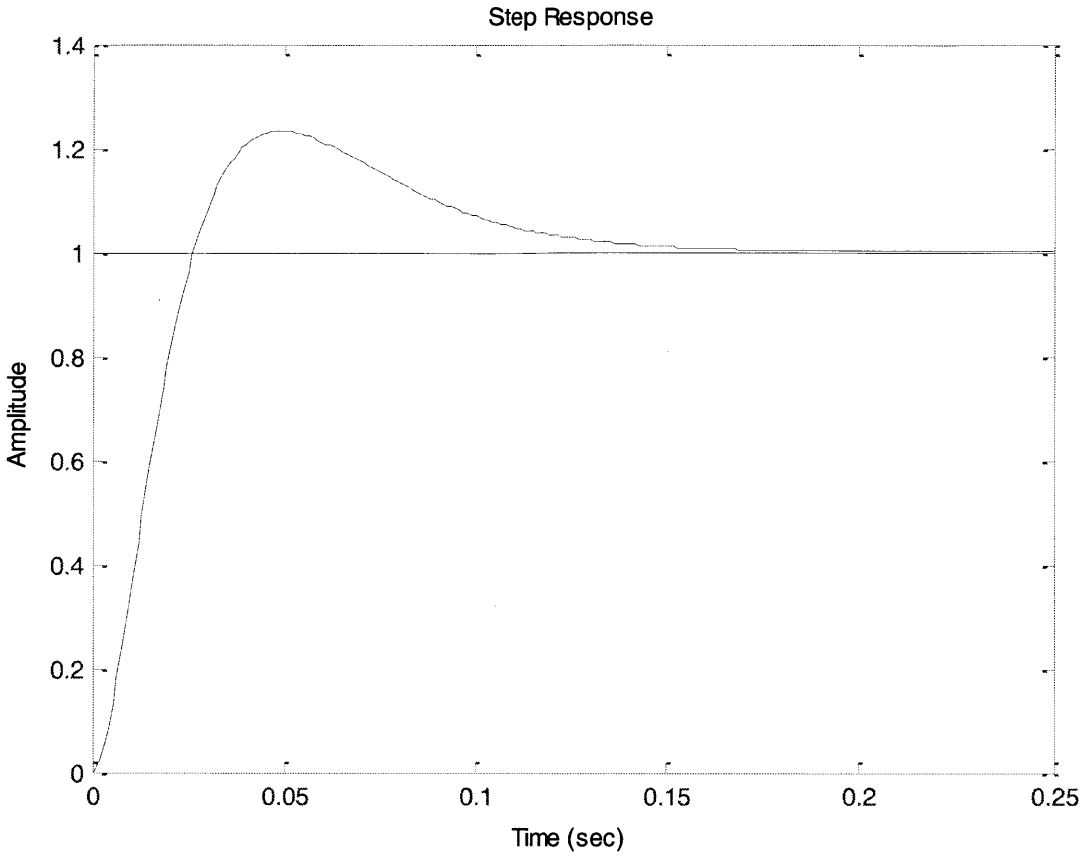

Figure 23: Simulated closed loop step response of feedback linearized system with lead compensation in the forward path; model given by Equation 15 with K = 83, α = 10, and τ = 0.005.

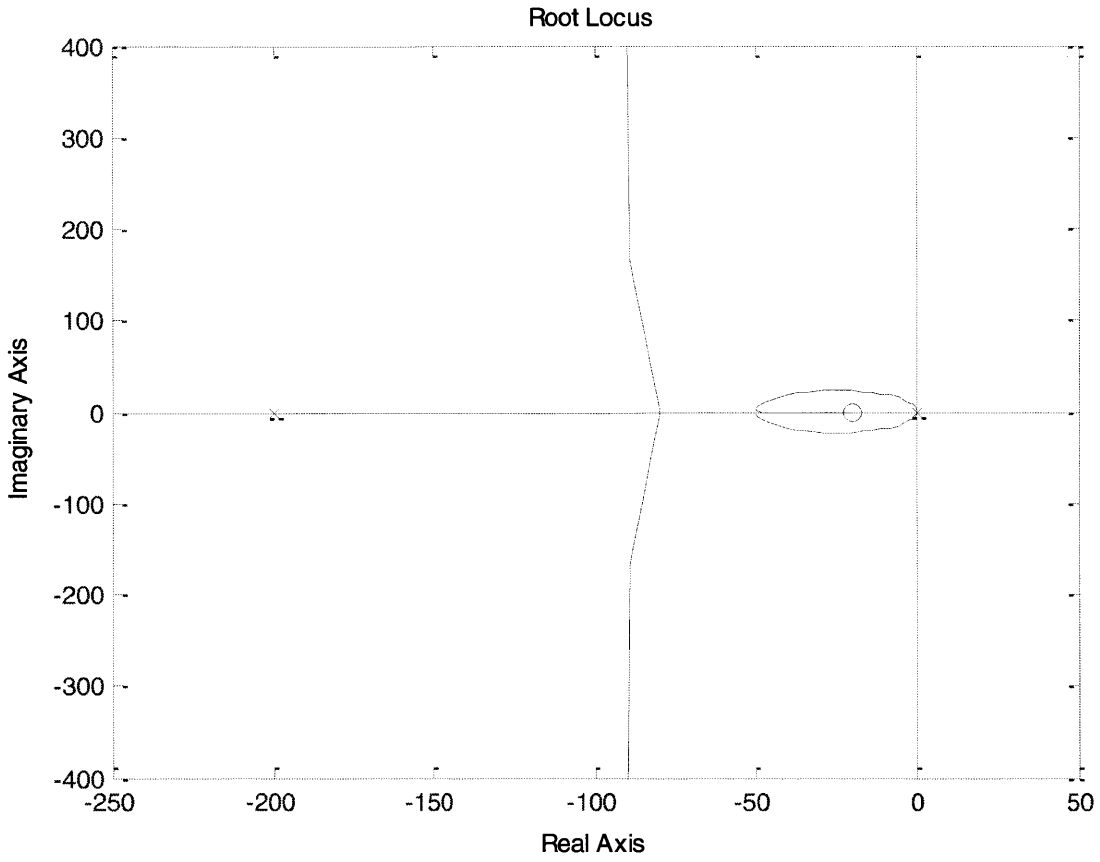

Figure 24: Root locus plot of suspension system with lead compensation.

The step response of the system has a small overshoot due to a closed loop zero. As seen in the root locus plot, shown in Figure 24, as the gain increases, the poles at the origin leave the real axis, circle around the lead compensator zero, and then one of the poles goes into higher frequencies while the other moves towards the zero from the compensator. At $K = 83$, one of the poles is at this low frequency zero that causes the overshoot seen in Figure 23. Thus, by moving the controller into the feedback path, poles in the feedback path become closed-loop zeros without affecting the loop transmission. This way, the closed-loop zero will move to a higher frequency and eliminate this overshoot. Figure 25 shows the closed-loop step response for the feedback linearized system with the lead compensator in the feedback path.

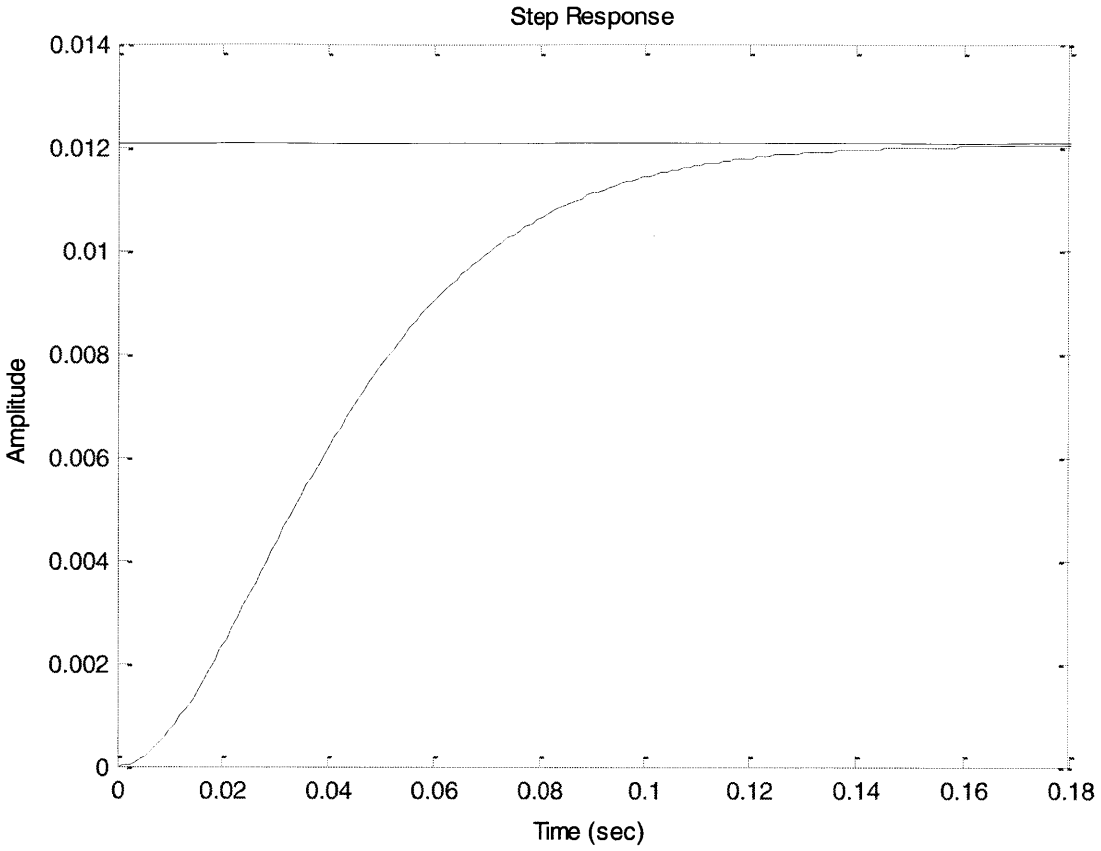

Figure 25: Simulated Closed loop step response of feedback linearized system with lead compensation in the feedback path; model given by Equation 15 with K = 83, α= 10, and τ = 0.005.

As seen in the new step response in Figure 25, we have eliminated the overshoot by gaining a steady-state error. Thus, we designed and implemented a lag compensator with an integrator to eliminate this steady-state error. For this case, we also placed the lag zero a decade before the crossover frequency, at 5 rad/s, and the pole at the origin. The simulated frequency and step responses are shown in Figure 26 and Figure 27, respectively.

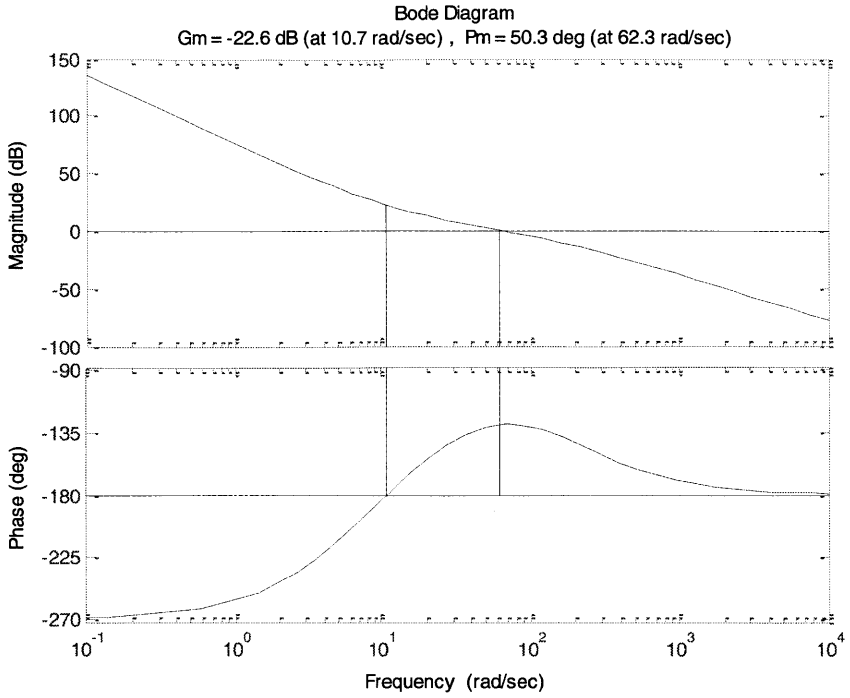

Figure 26: Simulated Bode plot for loop transmission of feedback linearized system with lead compensation in feedback path and lag compensation in forward path.

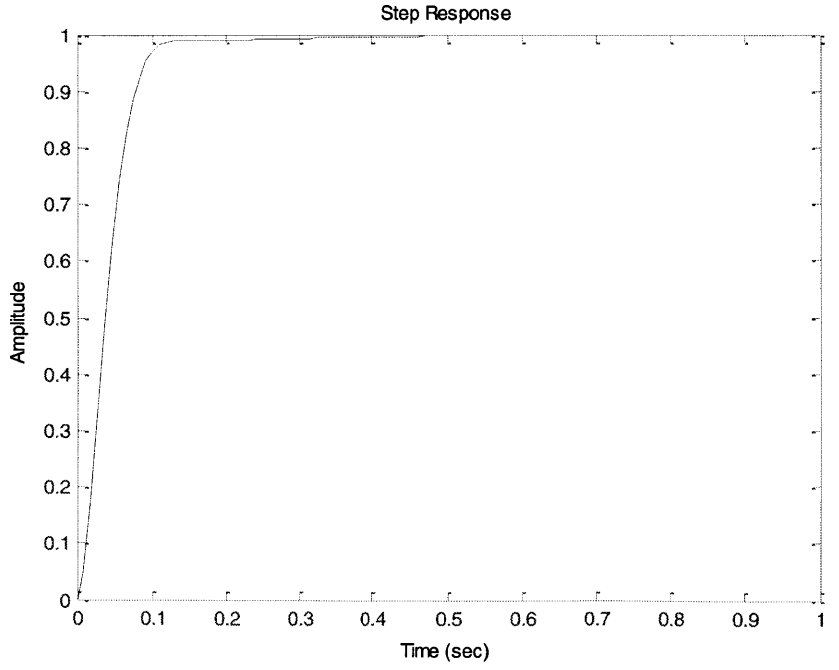

Figure 27: Simulated closed loop step response of feedback linearized system with lead compensation in the feedback path and lag compensation in forward path.

3.2.3 Controller Implementation

The lead compensator was implemented into the system through Simulink, MATLAB, and the dSPACE board. Figure 28 shows the Simulink model used for the controlling the feedback linearized system. In this system, the weight of the ball, which is the desired force the electromagnet must produce to counteract gravity, is subtracted because the desired force is in the negative direction. Also, the nonlinear transformation block implements Equation 5 to accurately find the desired current given the instantaneous force and gap length. Similarly to what happened when implementing the controller for the linearized model, the calculated gain based on simulations made the system unstable. Through experimentation, we noticed that gain for stability varied on the desired air gap, but it wasn't as sensitive as it was with the linearized system. For this controller, we used gain of 50 for air gaps between 4 mm and 11 mm and gain of 90 for the range 11-15 mm. In order to address the same noise issues, we implemented the same low-pass filter to the feedback linearization controller.

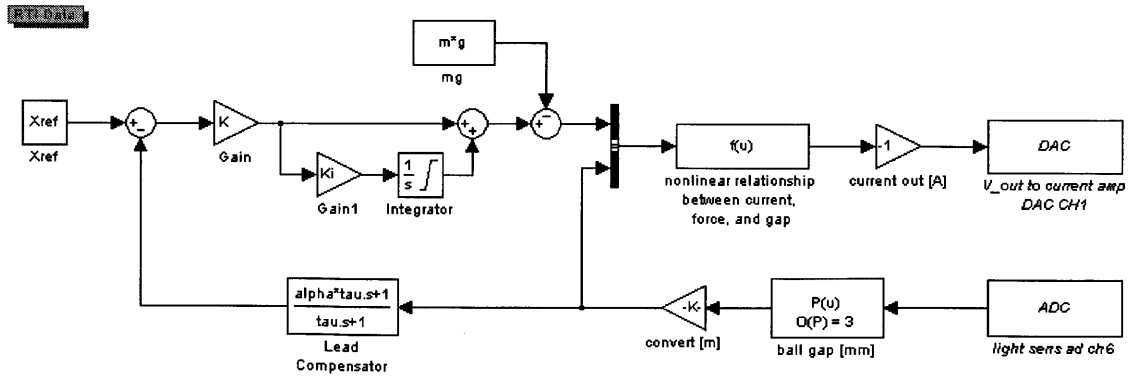

Figure 28: Simulink block diagram used to implement the controller for feedback linearized system.

Figures 29, 30, 31, 32, 33 and 34 show the system's postion responses to a 0.5 mm step at air gaps of 5 mm, 6 mm, 7 mm, 8 mm, 9 mm, 10 mm, 11 mm, 12 mm, 13 mm, 14 mm, and 15 mm. Like previously explained, we had to adjus the gain for air gaps of 11 mm or greater. However, unlike for the controller designed using linearization about an operating point, feedback linearization allowed the controller to be valid for greater ranges of air gap. With the same gain, we were able to have stable suspension rangin from 5 mm to 11 mm, although at 11 mm there was considerable oscilation. We increased the gain at this air gap and continued using it for greater air gaps. Interestingly, step responses seem to improve as air gap is greater; not only were the responses quicker and with less overshoot, but the signals were less noisy.

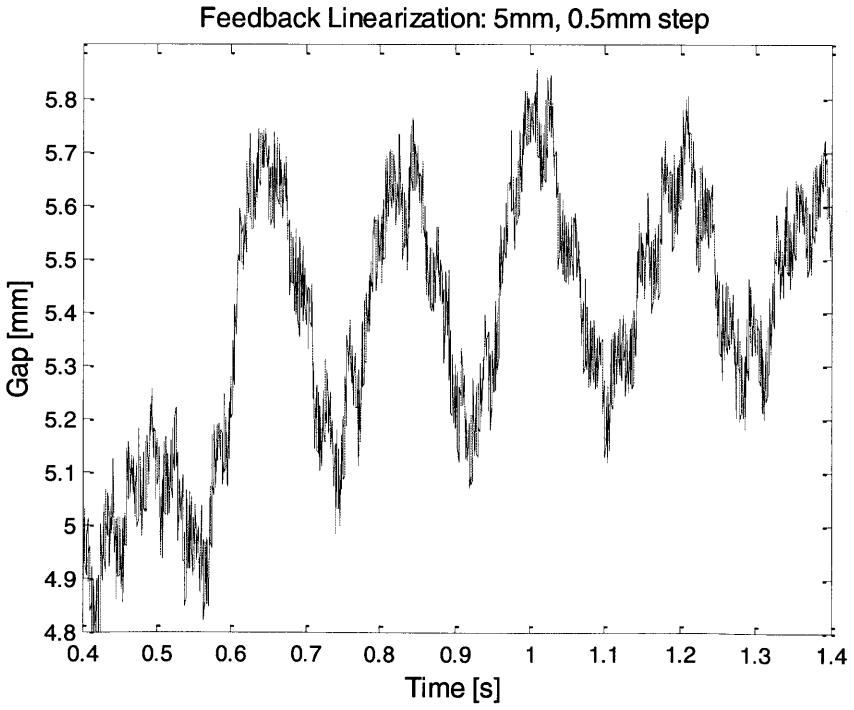

Figure 29: Position response as calculated from position sensor voltage measurement to a 0.5 mm step at 5 mm air gap (Feedback Linearization).

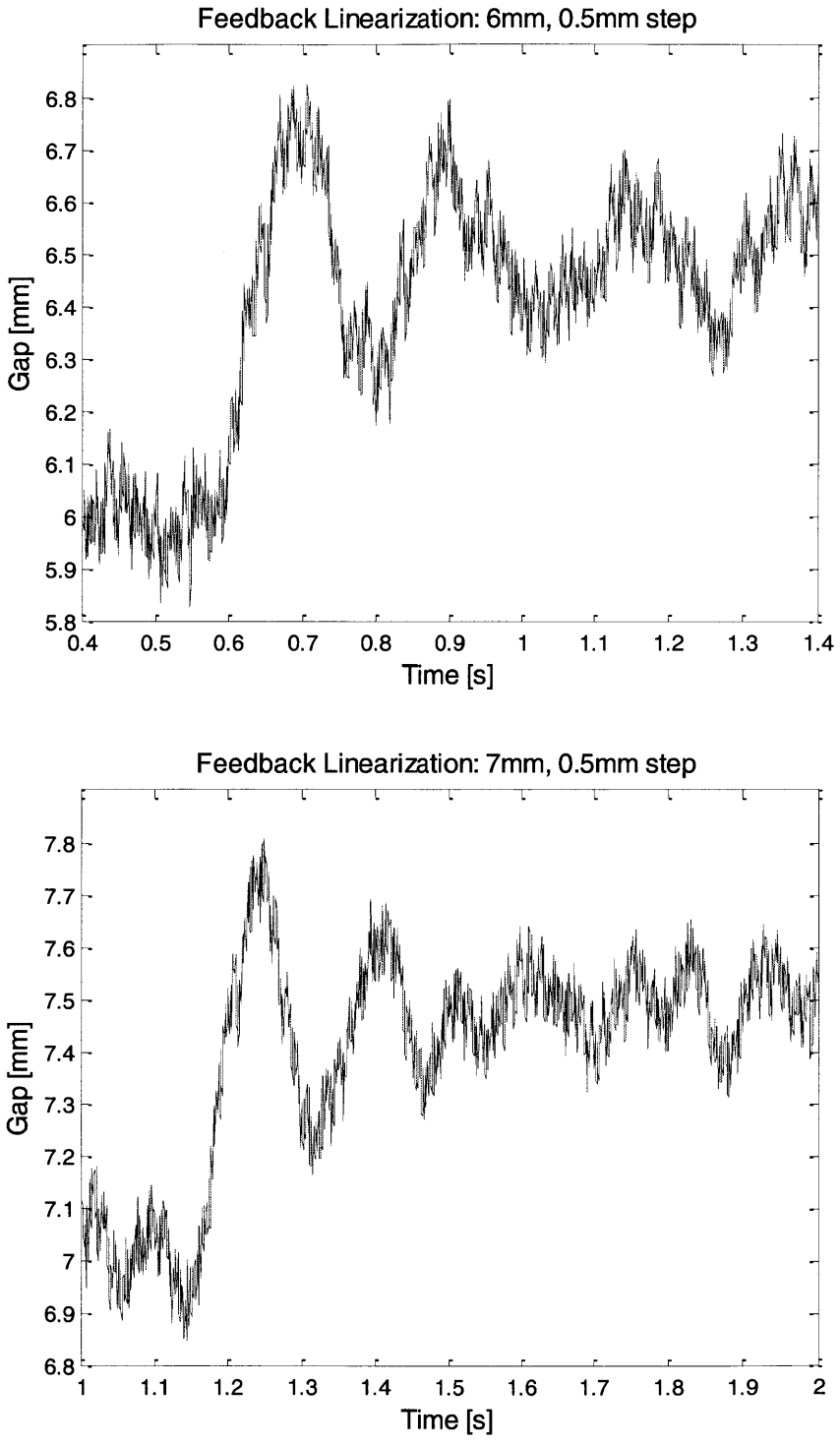

Figure 30: Position response as calculated from position sensor voltage measurement to a 0.5 mm step at 6 mm and 7 mm air gaps (Feedback Linearization).

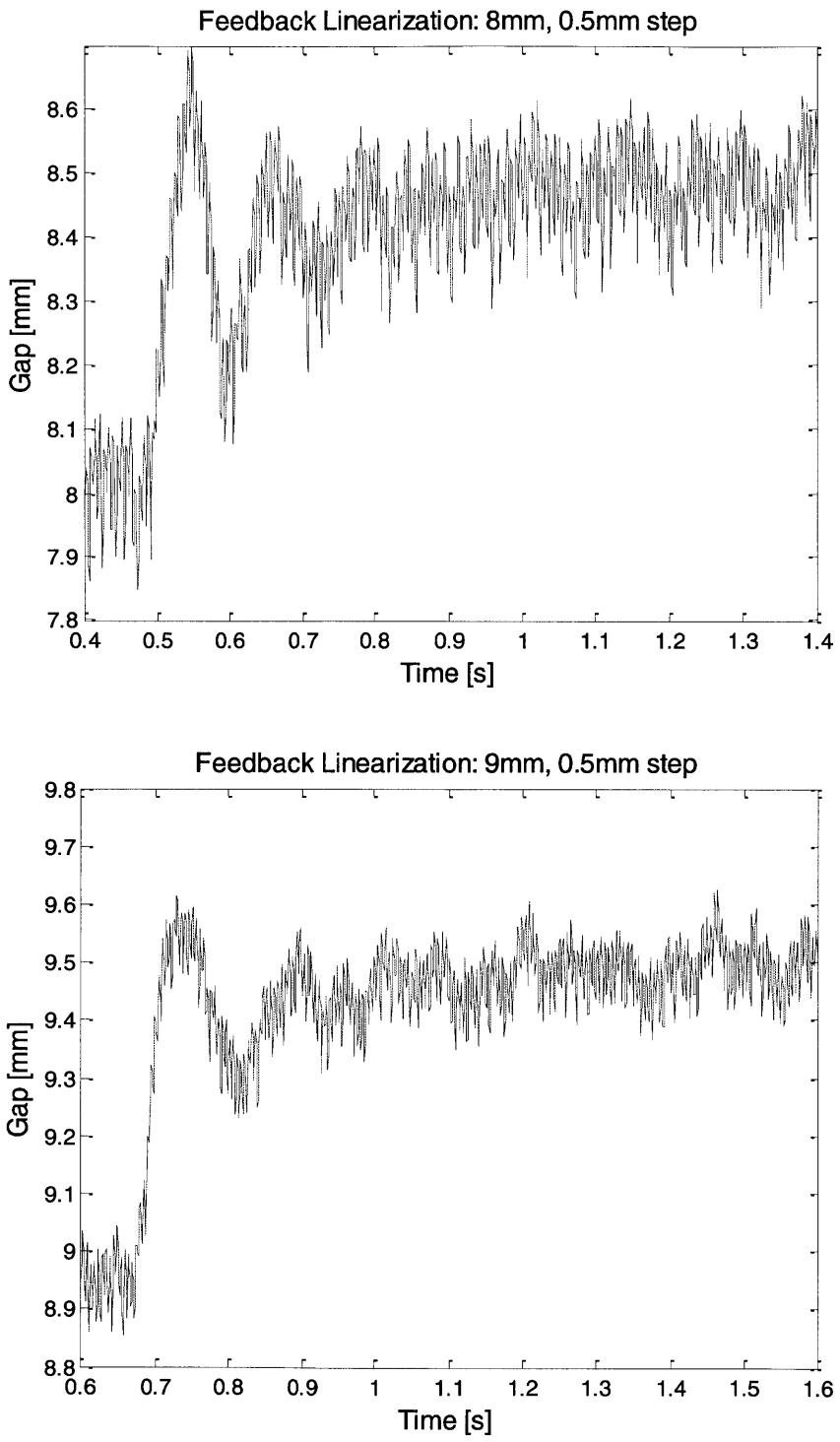

Figure 31: Position response as calculated from position sensor voltage measurement to a 0.5 mm step at 8 mm and 9 mm air gaps (Feedback Linearization).

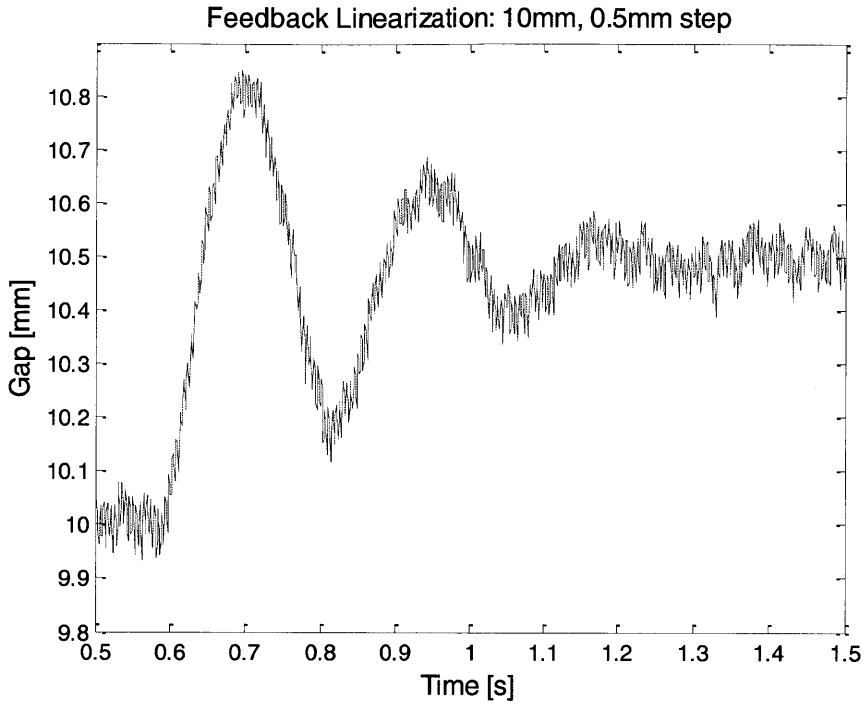

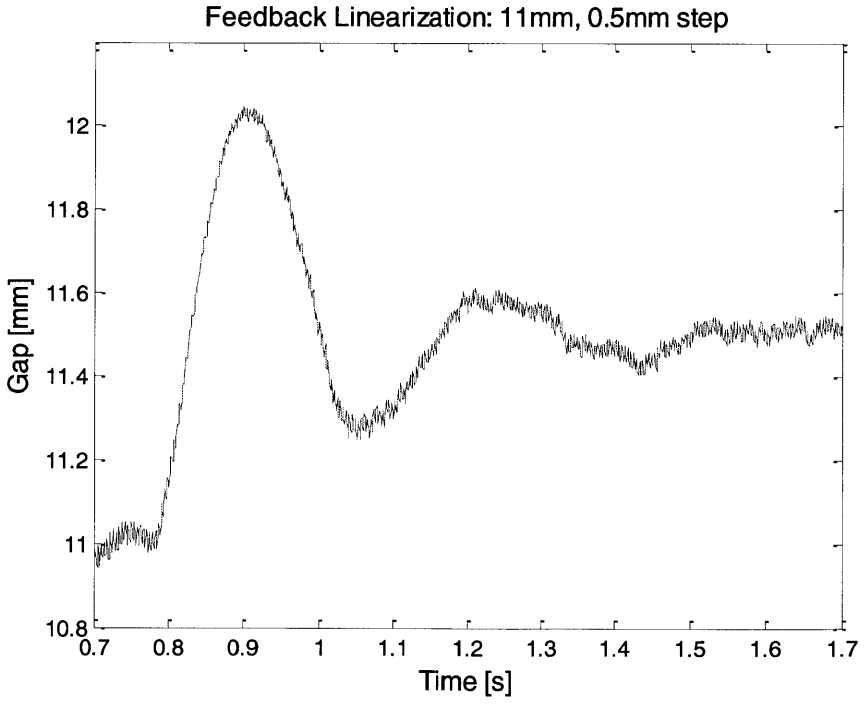

Figure 32: Position response as calculated from position sensor voltage measurement to a 0.5 mm step at 10 mm and 11 mm air gaps (Feedback Linearization).

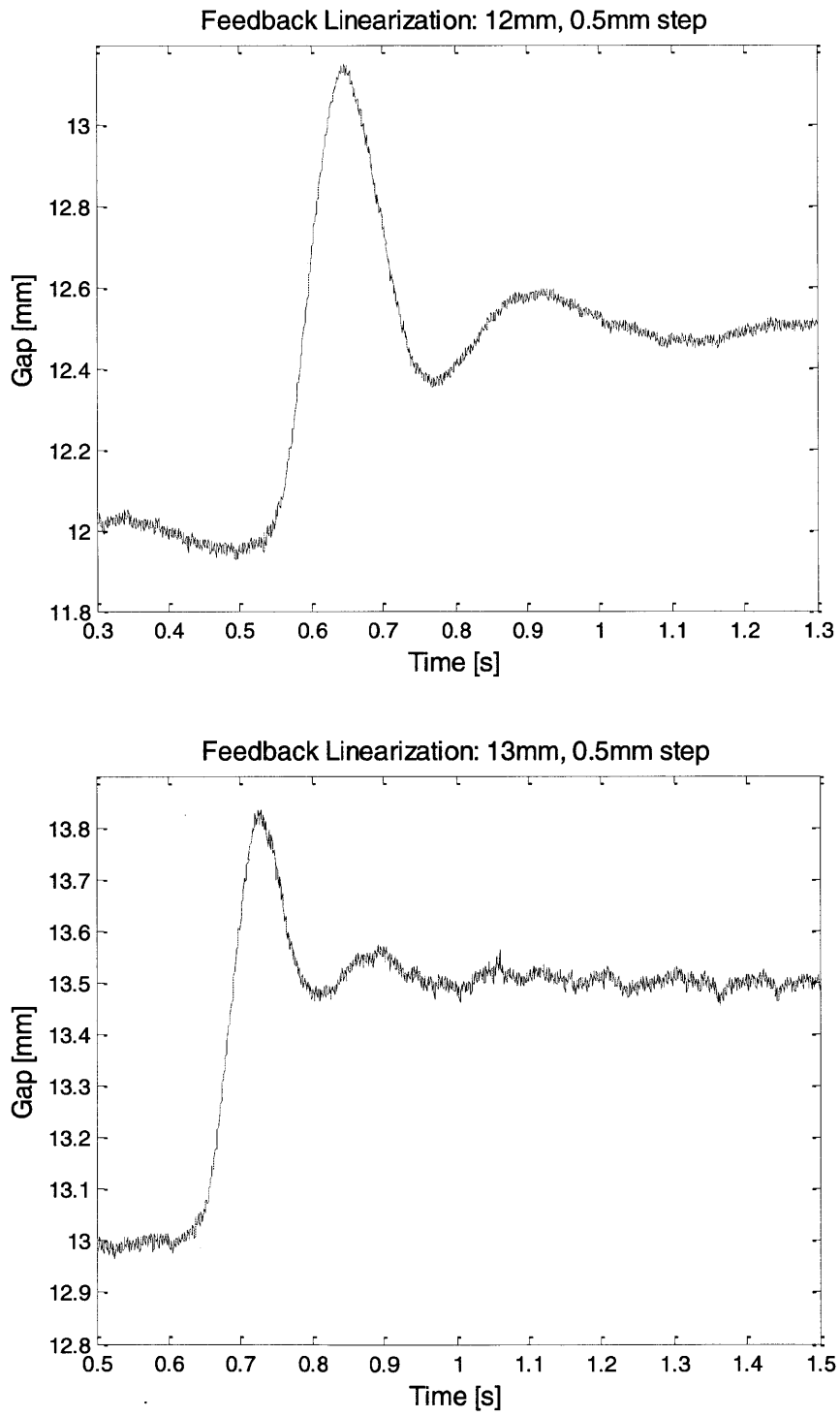

Figure 33: Position response as calculated from position sensor voltage measurement to a 0.5 mm step at 12 mm and 13 mm air gaps (Feedback Linearization).

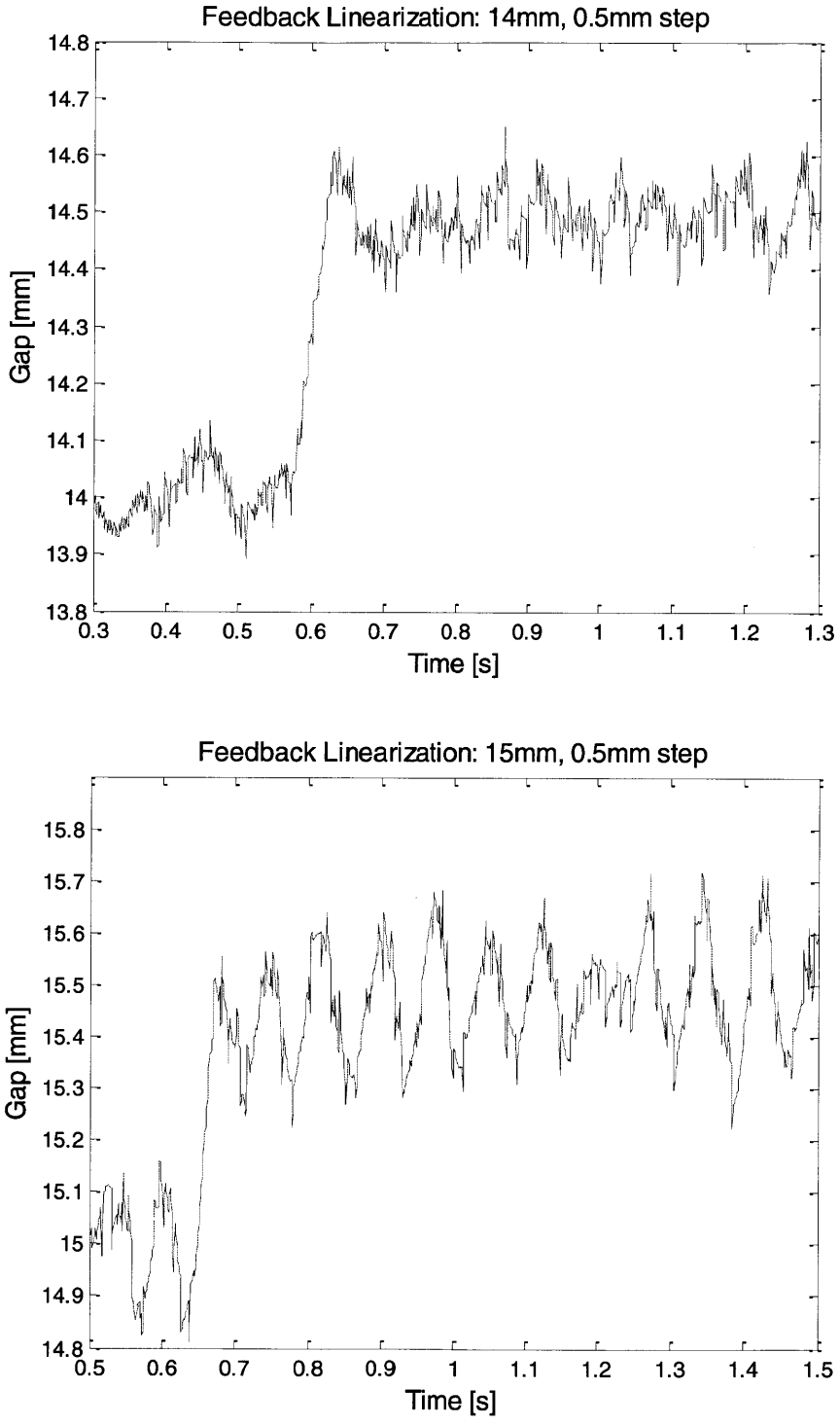

Figure 34: Position response as calculated from position sensor voltage measurement to a 0.5 mm step at 14 mm and 15 mm air gaps (Feedback Linearization).

3.3 Levitating Steel Ball

After successful implementation of two controllers uing different nonlinear control techniques, we were able to get the ball to levitate, as seen in Figure 35. The controller based on the linearized system uses simpler models, but has a limited range of validity. The controller based on the feedback linearization model operates accurately for a wider range of gap lengths at the expense of requiring higher levels of characterization.

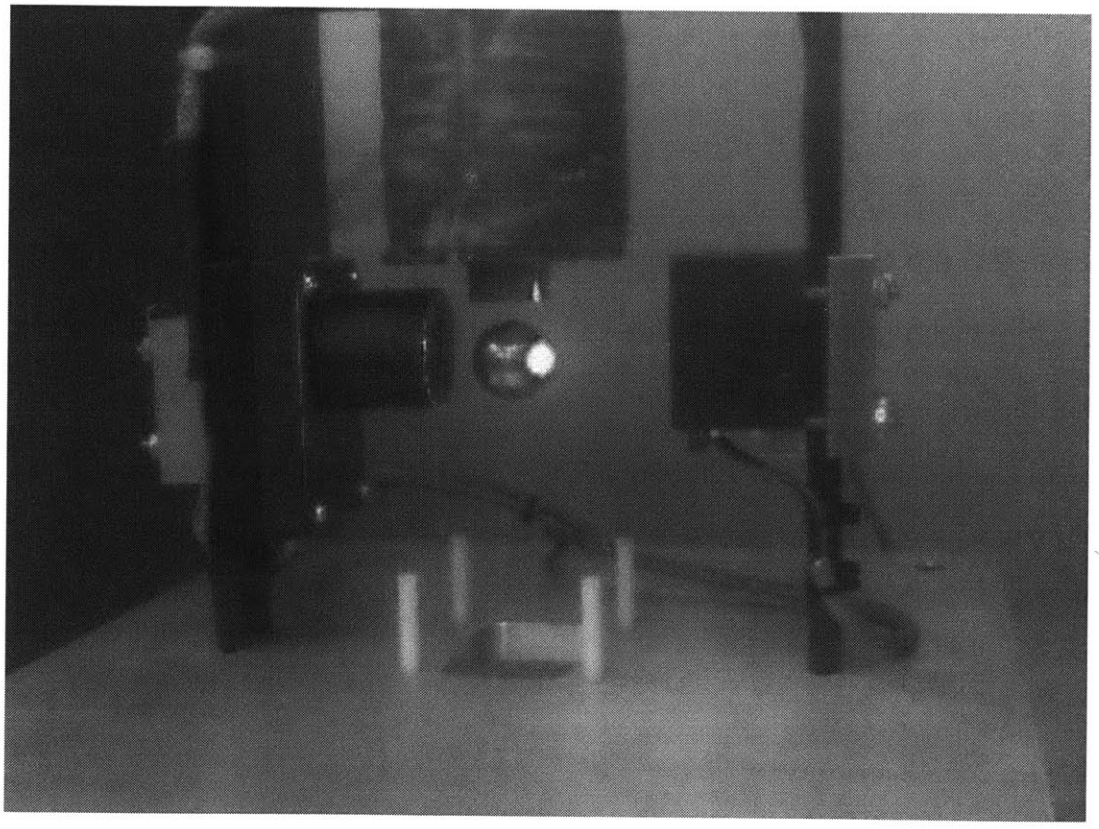

Figure 35: Photograph of steel ball in suspension.

Chapter 4: Conclusion

The thesis presented the design and implementation of feedback control tehniques for a naturally unstable system. The single-degree of freedom magnetic suspension device is an example of a classic nonlinear controls problem that required knowledge on modeling, dynamics, and nonlinear control techniques for the succesful implementation of a controller. After understanding the nonlinear nature of the single-axis suspension system, it was necessary to learn how to correctly use nonlinear control techniques: linearization around an operating point and feedback linearization. In addition, theoretical and experimentally fit models were developed for determining gap length from light sensor voltage readings and for relating force, current, and ball gap. A controller was designed using each approach to meet similar performance specifications. Throughout this process, we learned that while linearizing the plant about an operating point didn't require high order characterization of the electromagnet actuator, it had a very limited operating range. As for feedback linearization, it granted a nonlinear control independent of operating point on the expense of high sensitivity to modeling errors.

BIBLIOGRAPHY

1. Trumper D.L., Sanders J., Nguyen T., Queen M. *Experimental Results in Nonlinear Compensation of a One-Degree-of-Freedom Magnetic Suspension.* International Symposium on Magnetic Suspension Technology, 1991.

2. Xie, Y. *Mechatronics Examples for Teaching Modeling, Dynamics, and Control.* MS thesis, MIT, 2003.

3. Trumper D., Olson S., Subrahmanyan P. *Linearizing Control of Magnetic Suspension Systems.* IEEE Transactions on Control Systems Technology, Vol. 5, No. 4, July 1997.

4. Nise N. *Control Systems Engineering.* Delhi: Sareen Printing Press, 2009. Print.

5. Bosworth, W., Klenk D. *Nonlinear Control Technique Comparison for a Single DOF Magnetic Suspension.* 2.171 Final Project, MIT, 2009.